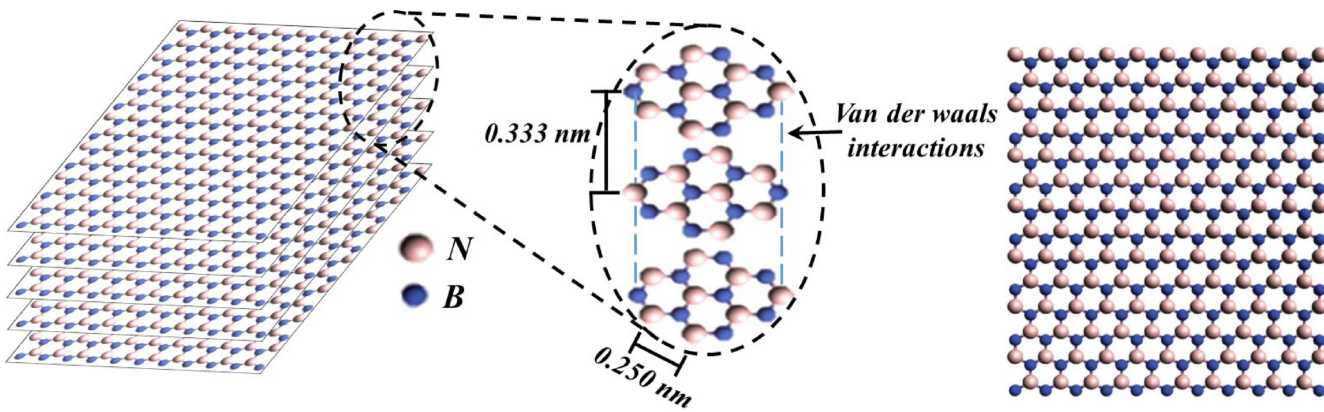


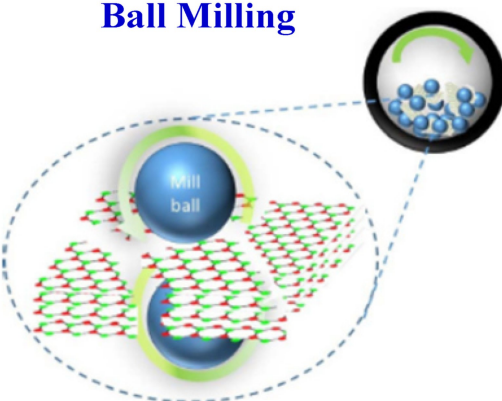


Advances in Studies of Boron Nitride Nanosheets and Nanocomposites for Thermal Transport and Related Applications

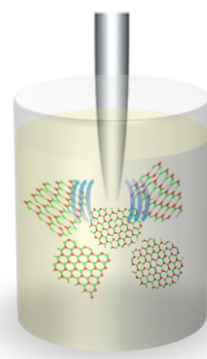
Mohammed J. Meziani,^[a, b] Kirkland Sheriff,^[a] Prakash Parajuli,^[c] Paul Priego,^[a] Sriparna Bhattacharya,^{*[c]} Apparao M. Rao,^{*[c]} Jesse L. Quimby,^[a] Rui Qiao,^{*[d]} Ping Wang,^[a] Shiou-Jyh Hwu,^[a] Zhengdong Wang,^[a] and Ya-Ping Sun^{*[a]}



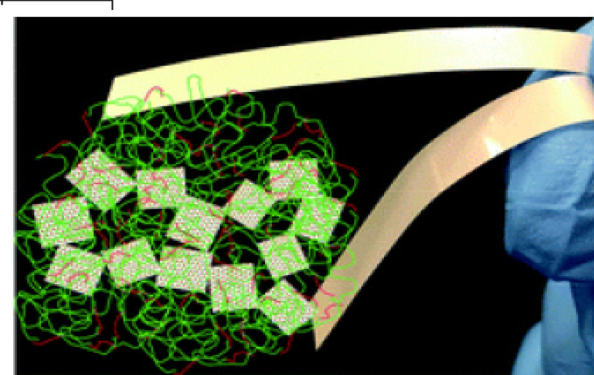
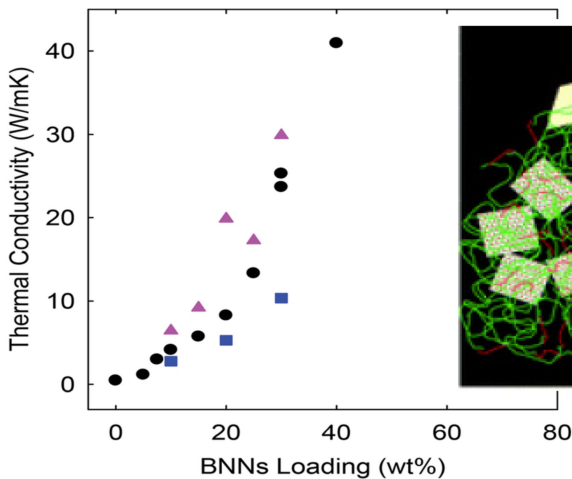
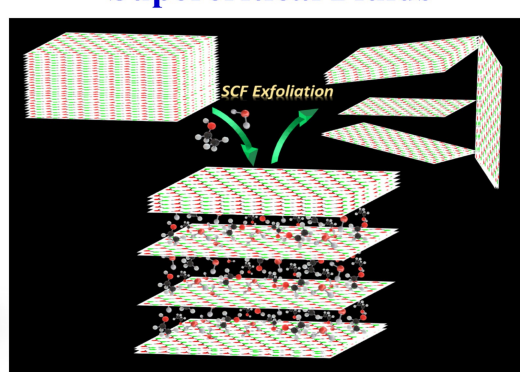
Ball Milling



Sonication



Supercritical Fluids



Hexagonal boron nitride (h-BN) and exfoliated nanosheets (BNNs) not only resemble their carbon counterparts graphite and graphene nanosheets in structural configurations and many excellent materials characteristics, especially the ultra-high thermal conductivity, but also offer other unique properties such as being electrically insulating and extreme chemical stability and oxidation resistance even at elevated temperatures. In fact, BNNs as a special class of 2-D nanomaterials have been widely pursued for technological applications that are

beyond the reach of their carbon counterparts. Highlighted in this article are significant recent advances in the development of more effective and efficient exfoliation techniques for high-quality BNNs, the understanding of their characteristic properties, and the use of BNNs in polymeric nanocomposites for thermally conductive yet electrically insulating materials and systems. Major challenges and opportunities for further advances in the relevant research field are also discussed.

1. Introduction

Hexagonal boron nitride (h-BN), often referred to as “white graphite”, is sp^2 -bonded two-dimensional layered material with a graphite-type structure in which planar networks of BN hexagons are regularly stacked.^[1–7] The B and N atoms are alternatively positioned to form planar conjugated layers, such that the two in the neighboring layers eclipse on top of one another because of the polarity mismatch. As a result, the slightly ionic bonding present in both in-plane and out-of-plane (so-called “lip–lip” interactions) in h-BN makes it different from graphite, such that the relatively stronger inter-layer interactions make the exfoliation of h-BN significantly more difficult than peeling off graphene from graphite.^[4–7] However, there are many unique and/or advantageous characteristics of BN, setting it apart from graphite. While both are among the best thermal conductors, BN is electrically insulating due to the wide bandgap, thus particularly valuable in uses that require or benefit from the decoupling between thermal and electrical conductivities. BN is also known for its remarkable properties, especially for being extremely stable both thermally and chemically with high oxidation resistance and passivity to reactions with acids and melts.^[8–12] More specifically, the graphite oxidation in the air starts at 400–450 °C, yet BN is stable at temperatures up to 1,000 °C in air and 1,400 °C in vacuum.^[11,12] BN is insoluble in commonly used acids, and in fact, only a few substances such as molten alkalis and alkaline solutions could attack or dissolve BN at elevated temperatures.^[11,12] Thus, BN is particularly valuable to uses under extreme conditions, such as in oxidative environments at very high temperatures.^[11,12]

The excitement associated with the single- and multi-layer graphene nanosheets has stimulated a similar intensive interest in few-layer BN nanosheets (BNNs, Figure 1)^[7] for their different properties from those of graphite and h-BN, respectively. BNNs retain the advantageous characteristics of h-BN, yet at the same time possess the desired features of nanomaterials, such as large 2D aspect ratios and solvent dispersibility, making BNNs excellent nanoscale fillers for polymeric nanocomposite materials.^[6,7,13–25] In fact, there have been extensive recent investigations on the development of polymer/BNNs nanocomposites for thermal management and other applications.

This review highlights the significant advances since our previous review in 2015^[7] on studies of BNNs and their derived polymeric nanocomposite materials for thermal transport and related applications. We emphasize new approaches and breakthrough developments of BNNs, and identify major challenges and related opportunities. Only the preparation of BNNs by exfoliation of h-BN is covered here, so readers interested in BNNs from “bottom-up” approaches may refer to other relevant and representative publications.^[6,15,16,26–31]

2. Preparation/Production of BNNs

Most BNNs have been prepared by the exfoliation of h-BN, conceptually and experimentally analogous to the exfoliation of graphite for graphene nanosheets, despite the fact that the former is generally more difficult due to the stronger inter-layer interactions in h-BN. Many processing approaches, methods, experimental protocols, and special processing conditions for the exfoliation of h-BN have been developed.^[6,7,15–17,26–29,32] Here, some of the more popular approaches, methods, and recent efforts are highlighted. Those designed more specifically for incorporating BNNs in certain polymeric nanocomposites are discussed in the next section.

2.1. Sonication in Selected Solvents

Exfoliation is a process driven by external energies delivered in different ways, which define the different exfoliation approaches.^[6,7,15–17,26,29,32] Vigorous sonication in selected solvents to deliver the required energy represents one of the most popular processing methods for exfoliating h-BN into BNNs. This technique has been applied independently or in combination with other energy delivery processes or with other

[a] Prof. M. J. Meziani, K. Sheriff, P. Priego, J. L. Quimby, P. Wang, Prof. S.-J. Hwu, Z. Wang, Prof. Y.-P. Sun
Department of Chemistry, Clemson University
Clemson, South Carolina 29634, USA
E-mail: syaping@clemson.edu

[b] Prof. M. J. Meziani
Department of Natural Sciences, Northwest Missouri State University
Maryville, Missouri 64468, USA

[c] P. Parajuli, Dr. S. Bhattacharya, Prof. A. M. Rao
Department of Physics and Astronomy, Clemson Nanomaterials Institute,
Clemson University, Clemson, South Carolina 29634, USA
E-mail: bbhatta@g.clemson.edu
arao@clemson.edu

[d] Prof. R. Qiao
Department of Mechanical Engineering,
Virginia Polytechnic Institute and State University
Blacksburg, Virginia 24061, USA
E-mail: ruiqiao@vt.edu



Prof. Mohammed Jaouad Meziani received both his M.S. (1995) and Ph.D. (1999) degrees in chemistry from the University of Montpellier II in France. After post-doctoral research in the lab of Prof. Ya-Ping Sun at Clemson University and then as the research manager at KWS-Tech LLC, he started his independent academic career at Northwest Missouri State University in 2010. He is now a full professor at the university. His research is in the development of nanomaterials for optical, electronic, and biomedical applications.



Kirkland Sheriff received his B.S. degree in chemistry from Georgia Southern University in 2018. He is currently a graduate student pursuing his Ph.D. in chemistry at Clemson University. His research involves a novel crystallization technique which relies upon the use of electrochemical potential as the driving force, and the development of nanomaterials including carbon-based quantum dots.



Prakash Parajuli received his B.S. and M.S. degrees in physics from Tribhuvan University in Nepal. He is currently pursuing a Ph.D. degree in physics under the supervision of Prof. Rao at Clemson University. His research interest includes nanomaterials and related DFT calculations, and the use of high-temperature Raman spectroscopy to study anharmonicity in thermoelectric materials.



Paul Priego received his B.S. (2016) degree in chemistry from University of California Riverside. He was a graduate student under the direction of Dr. Ya-Ping Sun. His graduate studies focused on the use of few/single layered boron nitride nanosheets for uses in thermal management systems. He is currently a Process Chemist at Ortec Inc. in Piedmont, South Carolina, USA.



Dr. Sriparna Bhattacharya received her Ph.D. in Physics from Clemson University in 2003 and is currently a research assistant professor at Clemson University. She completed her post-doctoral tenure at the University of Tennessee and the University of Virginia before returning to Clemson. Her research interests include thermoelectric materials, nano-generators for energy harvesting, biomedical imaging and applications.



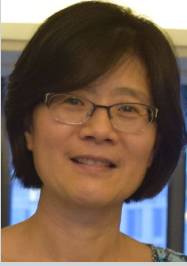
Prof. Apparao M. Rao received his B.S. degree (1982) in physics from the University of Mumbai, India, and his M.S. (1983) and Ph.D. (1989) degrees from the University of Kentucky. His research interests broadly encompass the synthesis, characterization, and applications of low-dimensional materials. He is the founding director of the Clemson Nanomaterials Institute and the Robert A. Bowen Professor of Physics in the Department of Physics and Astronomy at Clemson University. He is a Fellow of the American Physical Society, American Association for the Advancement of Science, Materials Research Society, and the National Academy of Inventors.



Jesse Quimby is currently a junior enrolled at The Citadel, the Military College of South Carolina. He is working towards a B.S. in both Mathematics and Physics with a minor in fine arts. He is interested in continuing his education in one of the engineering fields, including especially nuclear, chemical, and electrical engineering.



Prof. Rui Qiao obtained his Ph.D. at the University of Illinois at Urbana-Champaign in 2004. He was a faculty at Clemson University from 2005 to 2014 and joined Virginia Tech in 2014. His research focuses on interfacial and transport phenomena, and he has published on diverse topics such as nanofluidic transport, thermal transport in nanocomposites, electrical energy storage, and desalination.



Ping Wang obtained her B.S. degree in chemistry from Zhejiang Institute of Technology in China in 1983. She has been an independent researcher specialized in the preparation and characterization of novel materials, especially nanomaterials.



Dr. Shiou-Jyh Hwu (Ph.D. in Inorganic Chemistry, Iowa State University, 1985). His research is in the area of solid-state materials chemistry, including synthesis/characterization of inorganic solids and structure/property correlation studies of extended solids with unique properties. Research development includes low-dimensional solids, porous solids, narrow bandgap semiconductors, long-wavelength-infrared (LWIR) window materials, nonlinear optical (NLO) materials, nanostructured magnetic solids, superconductors, compounds with unusual oxidation states, and electrochemical crystal growth of conducting solids in aqueous solution.



Dr. Zhengdong Wang received his Ph.D. (2020) degree in electrical engineering from Xi'an Jiaotong University. He was a visiting Ph.D. student in the lab of Prof. Ya-Ping Sun at Clemson University (2018-2019). Since May 2020, he has been a faculty at Xi'an University of Architecture and Technology, currently an associate professor. His research interests include polymer-based composite materials for uses in thermal management and energy storage applications.



Prof. Ya-Ping Sun earned his Ph.D. at the Florida State University in 1989 and then got his postdoctoral training at the University of Texas at Austin until 1992, when he joined Clemson University faculty as an assistant professor of chemistry. He was promoted to full professor in 1999, and since 2003, he has been the endowed Frank Henry Leslie Chair Professor of Natural & Physical Sciences. His research interest is in materials chemistry and nanotech.

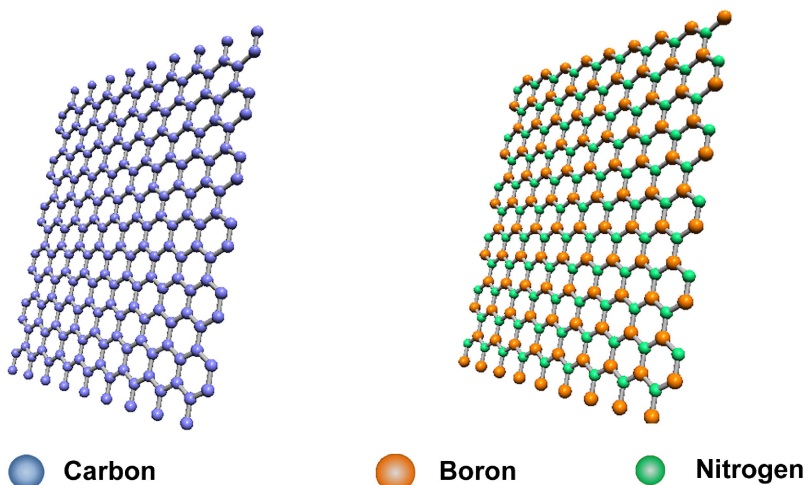


Figure 1. Graphene (left) and boron nitride nanosheet (right).

exfoliation approaches.^[26,29,32–79] For solution/liquid phase exfoliation in general, sonication always plays a major role in the overall processing.

On solvent selections for sonication, isopropanol (IPA) is often considered superior because of its experimentally observed more effective exfoliation outcomes.^[32–34] The good performance has been rationalized in part by using the Hansen solubility parameter theory, such that IPA has similar surface energy to that of the nanosheets, thus reducing the attractive van der Waals forces between the BN layers and the energy required for exfoliation.^[32,34] The exfoliation in IPA is usually coupled with vigorous sonication for an extended period to enhance the yields of BNNs. In a relatively minor modification to the processing protocol, the thermal treatment or refluxing of h-BN in IPA for 24 h followed by vigorous sonication was found to result in noticeably improved exfoliation outcomes, as reflected by the significantly more stable aqueous dispersion of the BNNs from the exfoliation (Figure 2, Table 1).^[33] The benefit of the thermal treatment step before sonication might be rationalized such that it could expand the interlayer gaps at the

edge defect sites of h-BN to enable easier penetration of the IPA solvent molecules during the vigorous sonication.

Similar surface energy match consideration has been applied to the selection of other solvents, including for example, *N*-methyl-pyrrolidone, 1,2-dichloroethane, *N,N*-dimethylacetamide, *N,N*-dimethylformamide, 1,2-dichlorobenzene, dimethylacetamide, and ethylene glycol, which coupled with vigorous sonication have generally resulted in relatively stable suspensions of BNNs.^[32–40] However, most of these are not favored solvents, due to their high cost, toxicity, high boiling point, etc., *versus* more desirable water and alcohols. Unfortunately, the latter with similar vigorous sonication have not yielded the desired exfoliation outcomes.^[41–43] In an alternative or modified approach, mixtures of the more desirable solvents have shown some promise.^[44–47] For example, the mixture of water with *t*-butanol or ethanol was found to improve exfoliation, as reflected by higher dispersion concentrations of BNNs.^[44–47]

Among other solvents evaluated for the dispersion and processing of h-BN with vigorous sonication have included

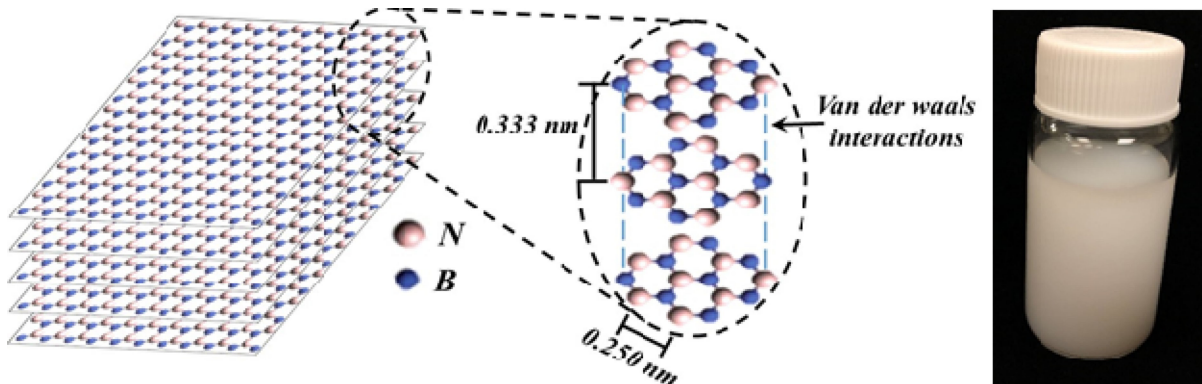


Figure 2. A schematic illustration on the crystal structure and some basic parameters of h-BN (left), and a photo of a stable aqueous suspension of BNNs obtained from refluxing and then vigorous sonication of h-BN in isopropanol (right).

Table 1. Exfoliation Methods, Conditions, and Outcomes.^[33]

Solvent	Treatments	Yield% ^[a] /Stability ^[b]
Water or DMF	48 h SN ^[c]	< 5%/Several days
IPA ^[c]	48 h SN	< 5%/Several days
IPA	24 h reflux & 48 h SN @50 °C	Up to 40%/Weeks
Water-DMF or IPA (1:1) ^[d]	48 h SN	< 5%/Several days
IPA-PEI (10:1)	48 h SN	< 5%/Somewhat stable
Water or IPA-Urea (5:1)	4 h SN	< 5%/Somewhat stable
Water or IPA-Jeffamine (10:1)	4 h SN	Trace/Unstable
5 M aqueous NaOH	72 h reflux	< 5%/Several days
H ₂ SO ₄ -HNO ₃	24 h SN	< 5%/Several hours
Aqueous ammonia-IPA (3:2)	48 h SN	Up to 20%/Weeks
Aqueous ammonia-IPA (3:2)	3 h @260 °C	> 20%/Stable
Milling w/PEI or Jeffamine, then water or IPA	3 h grind & 4 h SN	Trace/Unstable
Milling with urea, then IPA	3 h grind & 4 h SN	Up to 50%/Several days
Urea	20 h ball-milling & 24 h SN	> 30%/Weeks

^[a] The yield % measures the amount of dispersible exfoliated sample vs precursor h-BN. ^[b] The stability is for the dispersed sample against precipitation. ^[c] SN = sonication, and IPA = isopropanol. ^[d] Volume ratio for all mixtures.

those with Lewis base characteristics such as various amino molecules that were considered advantageous for their potentially binding with the electron deficient boron sites, thus to build upon the previously reported functionalization and solubilization of BN nanotubes by long-chain amine molecules^[48] and also the functionalization-assisted exfoliation of h-BN.^[33,49–53] However, the perceived advantage was found to be rather limited.^[33,53] For example, in a recent screening of various solvents containing amine moieties, including oligomeric polyethylenimines (PEI) and several Jeffamines (148, 220, and 230 in molecular weight), the outcomes were mostly no better in any major ways than those from the same exfoliation processing without the amino molecules (Table 1). For example, the Jeffamines in the absence or presence of IPA did not show any obvious advantages, though PEI was slightly more effective, especially when combined with IPA (such as in a PEI-IPA 1:10 v/v mixture).

There have been efforts on the use of surfactants,^[54–61] polymers and biopolymers,^[13,62–73] and large aromatic molecules,^[74–79] mostly in aqueous media, to improve the exfoliation. For example, sodium cholate and sodium deoxycholate surfactants were found to slightly improve the h-BN exfoliation in water with vigorous sonication, resulting in more concentrated and stable dispersions of exfoliated BNNs.^[54] In a more systematic comparison between groups of anionic, cationic, and nonionic surfactants,^[61] nonionic surfactants of larger molecular weights were found to be relatively more effective in terms of yielding more concentrated dispersion of BNNs, but the quality of the nanosheets was not so desirable. The conclusion from the study was that the role of the surfactants was primarily in the stabilization of the products from the exfoliation processing in aqueous dispersions, not so much in the exfoliation process itself. This is consistent with findings from other investigations in which some of the same surfactants were evaluated, suggesting that surfactants are generally ineffective in affording high-quality BNNs.^[57,60]

Conceptually similar has been the use of polymers and biopolymers in water or organic solvents in the exfoliation processing.^[19,62–73] Among popular polymer choices have been

polyvinylpyrrolidone (PVP), poly(vinyl alcohol), poly(styrene-*b*-methyl methacrylate), poloxamers, etc.^[62–73] The idea behind the use of polymers was to explore the possible steric effect, such that the hydrophobic groups of the polymer are partially adsorbed onto the basal plane of h-BN via π–π, hydrophobic, van der Waals, or charge transfer interactions, and at the same time, the hydrophilic groups are projected into the aqueous medium to provide effective repulsion.^[31,62–73] For example, PVP, selected for its popular use as a dispersant for other 2D materials, was added to water for the processing of h-BN to yield a more concentrated dispersion of the product, which contained few-layer nanosheets of relatively small lateral dimensions.^[62] Other polymers used for similar purposes have included polybutadiene, poly(styrene-*co*-butadiene), poly(vinyl chloride), poly(vinyl acetate), polycarbonate, poly(vinylidene chloride), cellulose acetate, polystyrene, and PMMA,^[63–68] though like the popular polymers discussed above the exfoliation outcomes were generally not exciting. The removal of the added polymers from the exfoliated samples could also become an issue in relevant applications unless the polymers are needed anyway, such as in nanocomposites of the corresponding polymers.^[64–68] For the use of biopolymers such as gelatin and nanofibrillated cellulose,^[69–73] the results and conclusions were largely similar to those with the use of synthetic polymers.

Molecules with large planar aromatic moieties have been explored for their expected π–π interactions with BN surfaces to aid the exfoliation and/or the stabilization of the exfoliated nanosheets in solvent dispersions.^[74–79] Among such molecules that have yielded interesting results are nickel phthalocyanine in *N*-methyl-pyrrolidone solution,^[74] 1,3-pyrenedisulfonic acid disodium salt in water,^[77–79] pyrene-conjugated hyaluronan,^[76] and *p*-phosphonic acid calix[8]arene.^[75]

The sonication in selected solvents is a simple approach for the exfoliation of h-BN, on which a wide variety of conditions and modifications have been investigated, as highlighted above. A critical and fair comparison of results from the different studies seems rather difficult due to the general lack of a set of experimentally easily accessible criteria or characteristic parameters, and also for the fact that many different

variables and processing conditions are involved. Nevertheless, all things considered it seems that the sonication in IPA still represents a relatively easy option in this simple approach, by which BNNs of reasonable quality and solvent dispersion characteristics can be obtained for their uses in thermally conductive polymeric nanocomposites and related materials.^[13,18–24,33] In this exfoliation approach, the modifications aimed at enhancing the exfoliation efficiency or replacing IPA with some more complicated or costly solvent systems have generally been not exciting, with a few achieving somewhat improved outcomes, but hardly considered transformational. Other exfoliation approaches have attracted significant recent attention, in which the sonication in IPA or other solvents has been incorporated as a step in the overall exfoliation processing.^[6,7,15–17,26,30,31]

2.2. Strong Acids and Bases

Strong acids such as H_2SO_4 or mixtures with H_3PO_4 or other acids, including also oxidants like $KMnO_4$ in the mixtures, were used with some success for the exfoliation of graphite into few-layer graphene nanosheets. The same approach typically coupled with vigorous sonication has been applied in the exfoliation processing of h-BN,^[33,53,80] though the outcomes have generally been much less satisfactory. In a more systematic exploration recently,^[33,53] the treatment of h-BN with concentrated H_2SO_4 or its mixture with HNO_3 , or by a strong oxidizing solution of $KMnO_4$ in concentrated H_2SO_4/H_3PO_4 at 50 °C followed by the addition of H_2O_2 , all coupled with vigorous sonication, was generally ineffective for the exfoliation.^[33,53] The dispersions of the resulting samples were unstable in terms of significant precipitations under ambient conditions over only a few hours at best. The dispersions could be made somewhat more stable by using harsher conditions in the treatment, such as high temperatures, but the corresponding samples were found to contain nanosheets in smaller sizes and with significantly damaged structures.^[81–85]

The apparently different outcomes of the same approach for the exfoliation of graphite *versus* h-BN may be explained by their different characteristics under strongly acidic and oxidative conditions. The structural and edge defects in graphite may be converted to oxygen-containing moieties, such as carboxylic acids, under the processing conditions,^[86,87] but the same is impossible with h-BN because of its highly stable nature. However, one may argue that the acid treatment of h-BN should be considered differently in terms of the protonation of the N sites, conceptually similar to the functionalization-assisted exfoliation.^[15,48–51] The observed generally poor exfoliation outcomes suggest that the protonation mechanism alone is insufficient. Similarly, the treatment of h-BN with strong bases such as concentrated NaOH, thus the “functionalization” of the B sites in h-BN, resulted in equally limited dispersion and exfoliation of h-BN.^[33,88–90] Therefore, even with the functionalization argument, the effects of strong inorganic acids and bases for their expected interactions with N and B sites, respectively,

must be insufficient to provide the kind of assistance for the desired exfoliation.

One recent approach based on the use of thionyl chloride as “solvent” for the exfoliation of h-BN, as reported by Lu and coworkers,^[91] may be considered with the acid effect in mind, because of the ready conversion of thionyl chloride into HCl. In the exfoliation processing, the sonication of h-BN in thionyl chloride for an extended period of time produced a milky dispersion that contained a significant amount of BNNs, with the estimated h-BN to BNNs conversion yield as high as 20%.^[91] The BNNs thus obtained were mostly on the order of 5 nm in thickness and a few hundreds of nanometers in lateral dimension (Figure 3), and they could be recovered by the removal of thionyl chloride and subsequently re-dispersed in various solvents such as acetic acid and 1,2-dichloroethane.^[91] Available experimental results have also suggested that the treatment of h-BN in thionyl chloride could introduce more structural defects, such as through-holes in the resulting nanosheets and a significant number of hydroxyl and amino groups on the surface or edges.^[92] Unlike the inorganic acids discussed above, strong organic acids such as the protic methanesulfonic acid and chlorosulfonic acid are apparently more capable of exfoliating h-BN,^[93–95] resulting in nanosheets of more defective structures. The BNNs thus obtained have found some interesting uses,^[91–95] though more broadly the structures and properties of these specifically processed nanosheets and their consequences to other applications remain an interesting topic for further investigations.

2.3. Mechanical Force Induced Exfoliation

A recently more popular approach has been the use of mechanical forces, specifically by ball-milling either independently or coupled with the pre- or post-treatment with vigorous sonication in selected solvents, to impart exfoliation of h-BN.^[33,53,96–108] Typically, the samples for ball-milling are mixtures of h-BN with selected organic molecules or bases such as aqueous NaOH.^[96–98] With molecules containing amine moieties mixed with h-BN, for example, the ball-milling of the mixtures in the solid state or as slurries is conceptually comparable with the use of similar amino molecules as dispersion-functionalization agents for h-BN in solution or suspension,^[33,99–102] except for the required energy delivered by the mechanical force in the former *versus* by sonication in the latter. Some of the representative studies and results reported in the literature are highlighted as follows.

Urea has been a popular choice in mixtures with h-BN for ball-milling,^[33,99] as rationalized such that the small urea molecules may be able to penetrate the interlayer defects in h-BN to aid the exfoliation. Typically with urea as the dispersion agent, the ball-milling produces amine-functionalized BNNs that are mostly thin but relatively small in lateral dimensions (less than 100 nm in many cases), forming concentrated and stable aqueous dispersions (Figure 4). Beyond urea, other organic compounds have also been explored, often with the consideration of their surface tensions being similar to that of

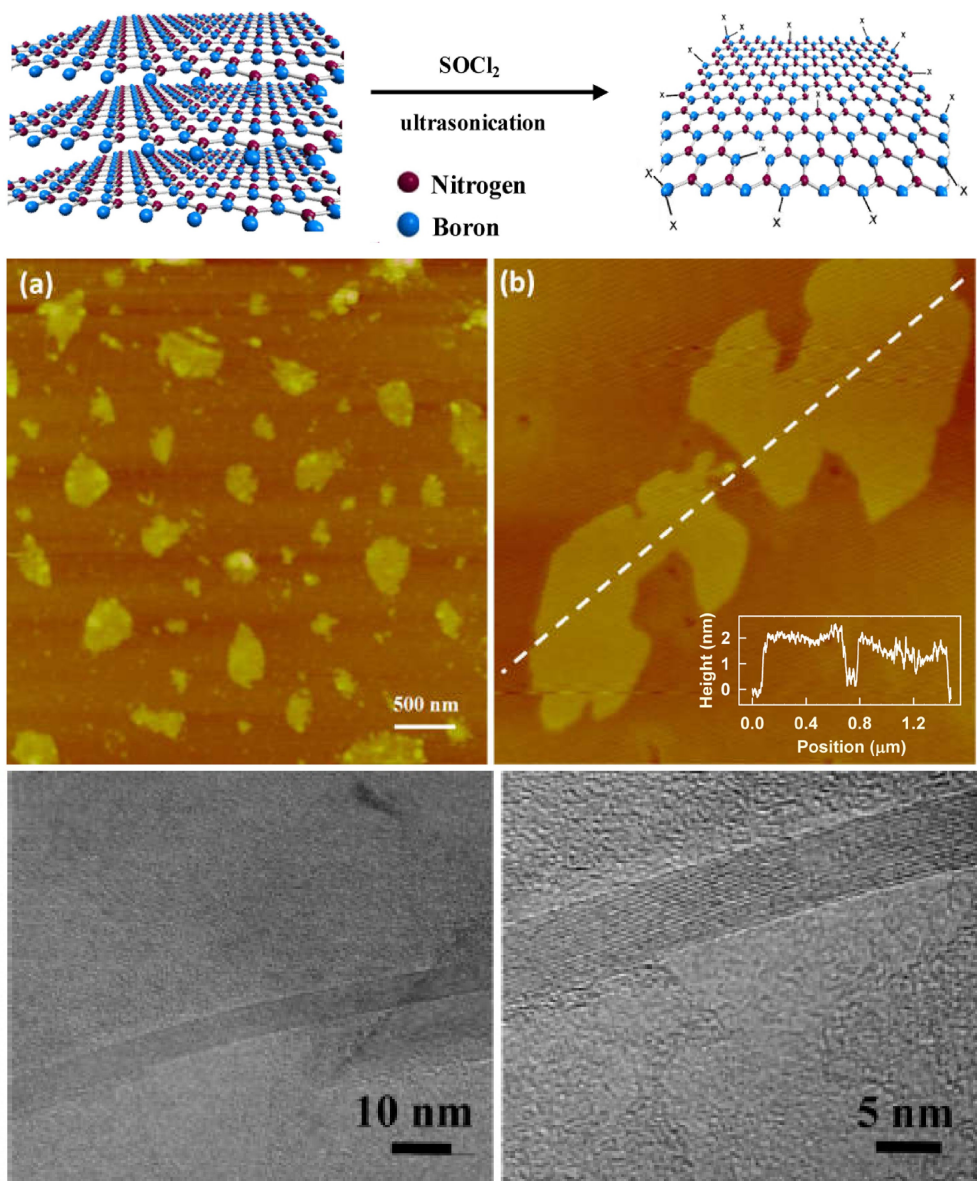


Figure 3. Top: A schematic for the preparation of BNNs by the exfoliation of h-BN in thionyl chloride. Middle: Topographic AFM images of the BNNs (a,b) and the height profile along the line of two nanosheets (the inset in b). Bottom: High-resolution TEM images on the folded edges of BNNs. “Reproduced/Adapted with permission from Ref. [91]. Copyright (2016) American Chemical Society”.

h-BN.^[103–108] For example, Li, *et al.* reported the use of wet ball-milling with benzyl benzoate, ethanol, and dodecane for gentle shear forces to cleave and peel h-BN.^[103] Lee and coworkers used ball-milling in the presence of aqueous NaOH, followed by sonication, to prepare OH-modified BNNs.^[96] Stable aqueous dispersions of OH-functionalized BNNs in high concentrations were also prepared with 2-furoic acid in the mixture with h-BN for the ball-milling.^[108]

The ball-milling aided by organic dispersion agents like urea, amines, and other molecules can apparently “break” h-BN into pieces pretty effectively, though the breaking may not be as selective as desired in the inter-layer direction for exfoliation. This may be understandable for the fact that h-BN is a layered ceramic in nature with significant inter-layer binding interac-

tions, and is generally considered brittle as well.^[109] The breaking of h-BN with strong external forces provided by ball-milling is analogous to that of using a hammer to break a multiple-layered ceramic china, yielding BNNs in small pieces (Figure 5) that may be different from the targeted nanosheets of a large aspect ratio. In a recent study,^[33] results on the sample of BNNs from the ball-milling in urea for 20 h, the processing conditions similar to those commonly found in the literature, followed by sonication in isopropanol for 24 h showed the consequence of the blunt external forces in the processing. The X-ray diffraction pattern of the sample was characterized by a substantial decrease in the (002) peak intensity from that of h-BN, accompanied by an increase in the peak width, suggesting the presence of abundant smaller pieces and defects. The assess-

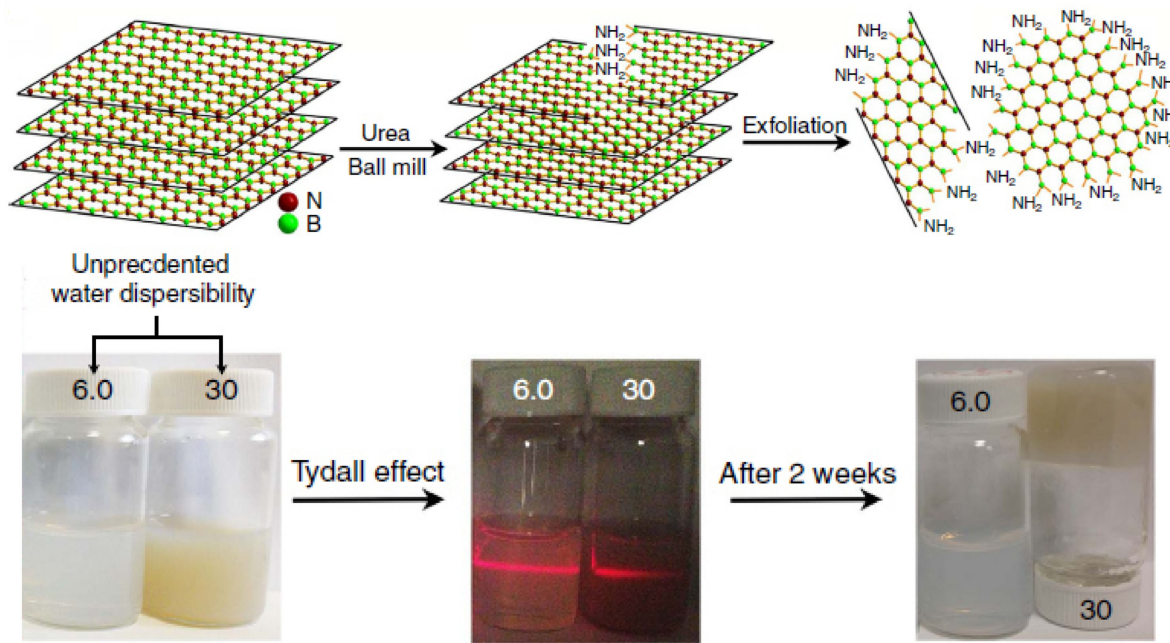


Figure 4. Top: A schematic for the preparation and functionalization of BNNs via urea-assisted ball milling. Bottom: Photos of BNNs suspensions in concentrations of 6.0 and 30 mg/mL. “Reproduced/Adapted with permission from Ref. [99]. Copyright (2015) Nature Publishing Group”.

ment was consistent with microscopy results (Figure 5), including the cross-sectional images of the nanosheets from the high-resolution TEM analysis and the finding of morphological probing by scanning electron microscopy.^[99] The relatively smaller BNNs, similar to those from the exfoliation in liquid thionyl chloride,^[53,91,92] may be suitable for some applications in which large lateral dimensions of the nanosheets are not so critical,^[99,10,111] but less desirable as fillers in polymeric nanocomposite films targeting high thermal transport performance.^[21,33,112]

The abundant experimental results on the exfoliation of h-BN by ball-milling have established the effectiveness of the method in terms of breaking up h-BN into nanosheets-like pieces, on which one may argue that the blunt mechanic forces applied to h-BN in ball-milling do more “breaking” inter-layer than cross-layer due to the intra-layer chemical bonds being much stronger than the inter-layer binding interactions. Such a differential in the binding strengths may be further exploited by better controlling the level of the mechanic forces, such as relatively weaker forces coupled with the selection of appropriate dispersion agents in the ball-milling, so as to enable more exfoliation-equivalent breaking to produce BNNs of both high aspect ratios and large lateral dimensions.

2.4. Ionic Liquids and Supercritical Fluids

Ionic liquids for their characteristic properties such as thermal stability, high polarity, and suitable surface energies have been explored for the exfoliation of h-BN.^[113–115] For example, the sonication of h-BN in ionic liquid 1-butyl-3-methylimidazolium

hexafluorophosphate yielded few-layer BNNs of micron-sized edges and good solvent dispersibility.^[113] The good exfoliation outcome was attributed to the strong cation–π interactions and charge transfers between the surface N sites in BN and the ionic liquid.

Supercritical fluids (SCFs) have been explored for their solvent properties particularly favorable to exfoliation, including low viscosity and high diffusivity, diminished surface tension enabling the easy access and penetration into small cavities, and extremely high compressibility.^[116,117] A popular and successful use of SCFs has been in extraction, yet both conceptually and practically, the solvent properties of SCFs special to extraction are equally beneficial to exfoliation. For example, the high diffusivity and vanishing surface tension in SCFs enable the solvent molecules to penetrate the interlayer spacing of layered materials for more effective and efficient exfoliation.^[33,118–122]

Among early demonstrations on the unique advantages of SCFs for exfoliation was the use of supercritical CO₂ in the direct intercalation and delamination of graphite.^[118] An added dimension with supercritical CO₂ for the exfoliation of graphite into graphene nanosheets is green processing,^[116,117,121] though the nonpolar nature of CO₂ has been found to be a significant limitation in achieving the desired exfoliation outcomes.^[119–122] Other SCFs, such as ethanol, DMF, or various solvent mixtures under supercritical conditions,^[119,122–128] have been investigated for the exfoliation, some of which yielded high-quality graphene nanosheets (Figure 6).^[123–128] The same approach and unique solvent properties of SCFs have naturally been considered and applied in the exfoliation processing of h-BN.^[33,129–133]

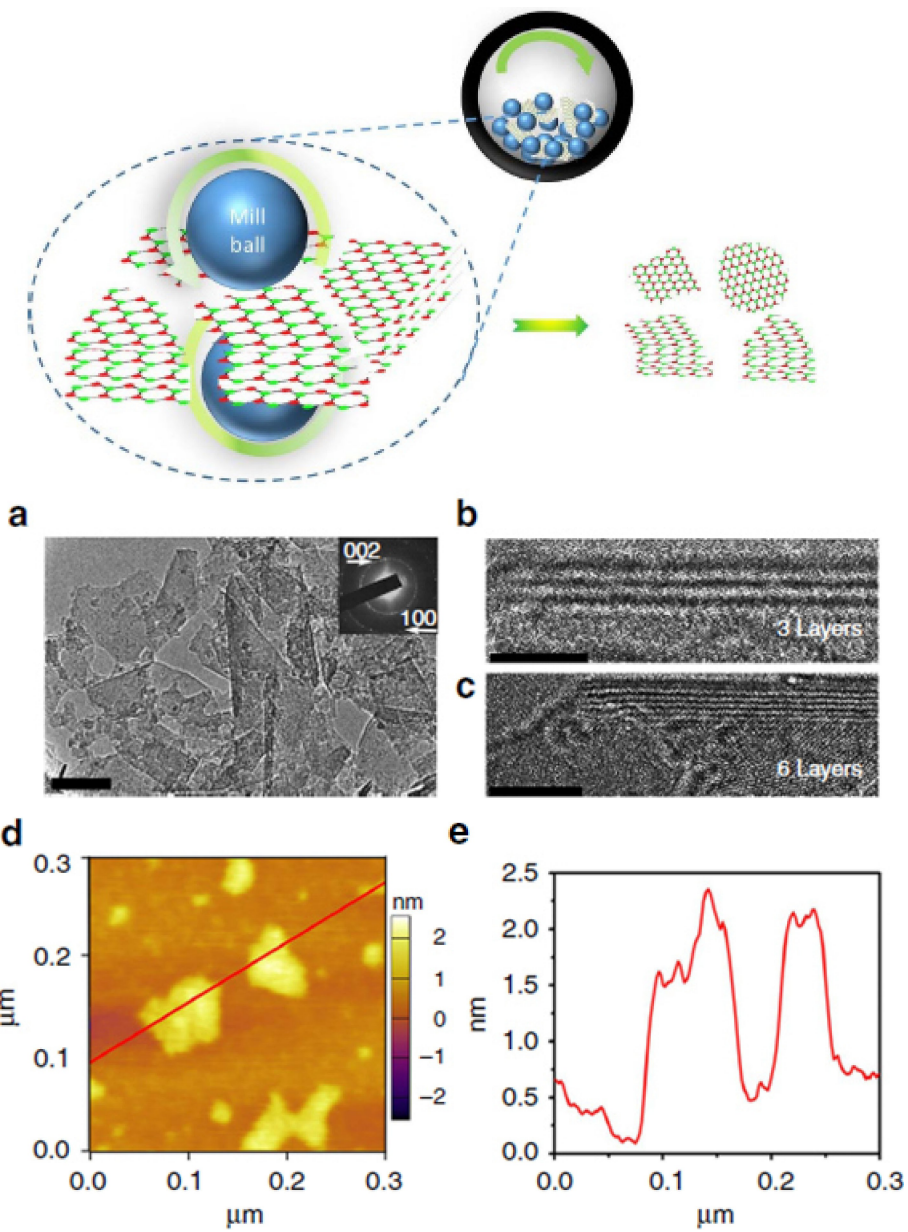


Figure 5. Top: A cartoon on what might be happening in the ball-milling of h-BN, probably more breaking by the strong shear forces (arrow) than exfoliation to yield BNNs-like small pieces. Middle: (a) TEM image (the scale bar of 50 nm) of BNNs from urea-assisted ball milling, with the selected-area electron diffraction pattern shown in the inset suggesting a layered BN structure. (b,c) High-resolution TEM images (the scale bars in b and c of 2 nm and 5 nm, respectively) on the folded edges of two pieces of BNNs. Bottom: Atomic force microscopy image (d) and the corresponding line-scan profile (e) of the BNNs. (Middle and Bottom, "Reproduced/Adapted with permission from Ref. [99]. Copyright (2015) Nature Publishing Group".)

For example, an isopropanol-water in equal volume fractions at 400 °C was used for the exfoliation of h-BN into few-layer nanosheets in high efficiency.^[132] In a more recent study, the ethanol-water mixture (70/30 v/v) at the processing temperature higher than the critical temperatures of both solvent components was found effective in the exfoliation of h-BN, yielding thin BNNs of larger aspect ratios and less defects (Figure 6).^[133] The supercritical processing was efficient, in terms of a relatively short processing time of 20 min for a high yield of the harvested BNNs. The XRD pattern of the exfoliated sample suggested no significant surface oxidation of the BNNs,

with the diffraction peak features consistent with thinner nanosheets without any substantial crystalline structural damages. The further assessment on the structural and morphological characteristics of the BNNs by scanning electron microscopy and high-resolution transmission electron microscopy imaging analyses confirmed that the nanosheets from the supercritical fluid exfoliation contained mainly thin BNNs of lateral dimensions in microns and generally of smooth surfaces and less defective edges,^[33,133] namely the characteristics generally desired and targeted by various exfoliation methods.

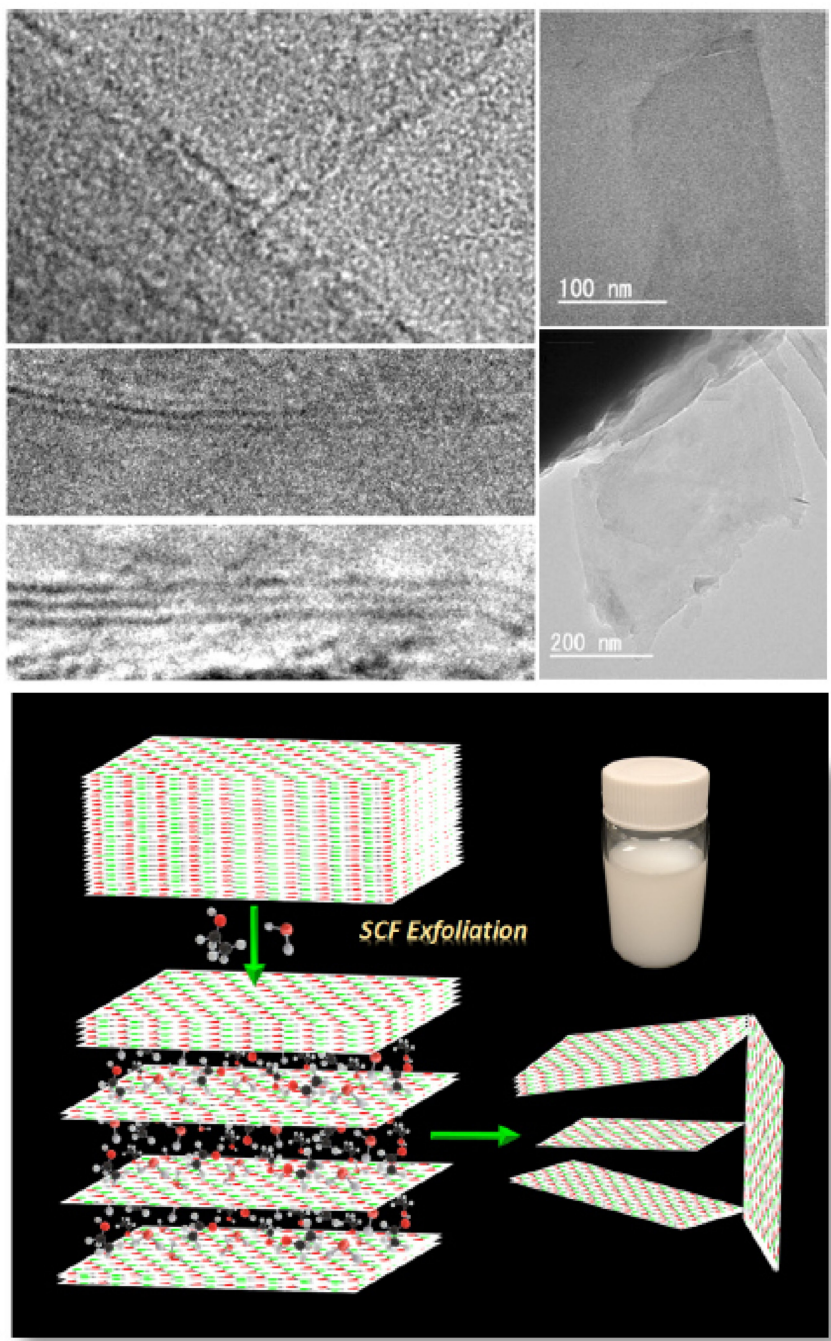


Figure 6. Top: TEM images of few-layer graphene nanosheets from the exfoliation of graphite in supercritical ethanol (left) and supercritical CO₂ (right). “Reproduced/Adapted with permission from Ref. [128]. Copyright (2020) Springer”. Bottom: A schematic illustration on the exfoliation in SCF processing of h-BN, with the photo showing a stable aqueous dispersion of the BNNs thus obtained. “Reproduced/Adapted with permission from Ref. [133]. Copyright (2021) Elsevier”.

Water is a green solvent, and alcohols are benign and recyclable post-exfoliation processing, but the utilization of supercritical CO₂ at lower processing temperatures also has significant benefits. Water-CO₂ mixtures have always been considered as the dream solvent system in almost all aspects of supercritical fluid processing.^[116,117] Due to the generally low miscibility of water with CO₂ at the desired low processing temperatures, surfactants or the like are often added for

emulsions to be used as the processing media.^[116,117,130] For example, CO₂/polyvinylpyrrolidone/(ethanol + H₂O) emulsions were used for the exfoliation of h-BN and other layered materials, in which some few-layer nanosheets were obtained.^[130] Alternative to the use of surfactants, which obviously adds complexity to the system and operation, supercritical CO₂ was coupled with other exfoliation forces, such as

the shear-assisted and ultra-sonication in supercritical CO₂ for the exfoliation of h-BN to yield some few-layer BNNs.^[129,131]

Ammonia is often considered as one of the near-ambient SCFs, with the critical temperature of 132°C, and it is simple amine-like. Its role and excellent potential in the exfoliation processing of h-BN have just begun to be recognized.^[33] In a recent systematic comparison of different exfoliation approaches and processing conditions (Table 1), the hydrothermal treatment of h-BN in the mixture of aqueous ammonia solution and isopropanol was identified as being more effective in the exfoliation for BNNs of desired characteristics.^[33] The contribution of ammonia to the observed effective exfoliation was rationalized as being due to a combination of electronic characteristics, small size, and lower polarity of ammonia at the processing temperature significantly higher than its critical temperature, thus enabling more specific molecular interactions and easier insertion into the h-BN inter-layers. The findings prompted the evaluation of supercritical ammonia for the exfoliation of h-BN, from which the results were very promising.

In general, SCFs with their unique solvent properties and the associated processing methods are conceptually and technically excellent choices for the exfoliation needs, enabling the production of high-quality BNNs in large yields. More experimental and also modeling efforts on the development of SCFs-based exfoliation processing are anticipated.

2.5. Technical Issues/Challenges

A major technical issue or challenge in the development of exfoliation methods for high-quality BNNs is the general lack of convenient and reliable characterization techniques for efficient evaluations of the exfoliation outcomes. Consequently, the relevant research community is missing a set of fairly comparable, as agreed and followed by different researchers developing and applying different exfoliation techniques and protocols in the field, specific structural and morphological parameters for any specifically prepared BNNs and their counterparts obtained from other exfoliation approaches. Among commonly employed are X-ray powder diffraction (XRD) and electron microscopy including scanning (SEM) and transmission (TEM). Since most of the exfoliation methods are associated with solvents, a quick screening to triage those with undesirable outcomes has been the poor solvent dispersion characteristics of the sample from the exfoliation processing, based on the implicit assumption that well exfoliated BNNs should form relatively more stable solvent dispersions. The validity of such an assumption may be subject to debate and experimental verification, but for many intended uses of BNNs, the poor or no solvent dispersion at all may prove problematic anyway. On the other hand, BNNs capable of forming stable solvent suspensions against precipitation may be favorable to some applications, but they are not necessarily correlated with well exfoliation in terms of fewer layers and large aspect ratios and/or less defective nanosheets.

XRD is a convenient technique for the characterization of BNNs in the solid state, looking at the broadening of diffraction peaks (Scherrer equation)^[134] and, to a lesser extent, the peak

shifts. There have been concerns on the possible changes in samples from as-exfoliated BNNs in solvent suspension to the solid state. The samples of exfoliated BNNs are often complex mixtures, whose effects on XRD results may make the correlations of the observed peak broadening and shifts with the quality of exfoliation more difficult, less consistent or quantitative at least. The comparison of the estimated average thickness of the BNNs from XRD peak broadening based on Scherrer equation with that determined by TEM imaging of the same sample (microtomed for cross-sectional view) is often required or preferred, though the latter may have its own shortcomings. The high-resolution TEM imaging of a microtomed sample slice looks at a very small area of only a few BNN cross-sections at a time, thus not so realistic with respect to the collection of a large number of images in nanometer resolution to match precisely the XRD results on BNNs in bulk.^[33,53] Assumptions will have to be made for the comparison between XRD and TEM results, for which the rigorous experimental verification is hardly an easy task.

There have been discussions and debates on what constitute "high-quality" BNNs and correspondingly effective exfoliation methods, namely on the desired features and properties of the BNNs from preferred exfoliation methods. The commonly held perceptions call for the effective exfoliation of h-BN into BNNs that are thinner in thickness and larger in lateral dimension, thus correspondingly higher aspect ratios, and smooth surfaces with less defects. These qualifications may be originated from investigations and results of graphene nanosheets, probably right in common sense, but still remain to be validated in carefully designed systematic evaluations. On the surface characteristics and defect population, they could be application dependent or specific. For the use of BNNs in thermally conductive polymeric nanocomposites discussed next, it seems that there have not been systematic efforts on quantitatively correlating the surface and edge properties of BNNs with the thermal transport performance of their derived polymeric nanocomposites, likely due to some major experimental challenges.

Generally speaking, the critical challenge for the relevant research community is the need to develop and agree upon the important material parameters of BNNs that can be shared fairly and reproducibly in evaluations of different exfoliation approaches and methods under varying processing conditions, which would require similar development and agreement on convenient and reliable experimental characterization techniques for various BNNs prepared via exfoliation. These will be the precursors for the broadly accepted more precise definitions on the "high-quality BNNs" and by extension the "effective exfoliation approaches and methods", even though the exact criteria could be different for different targeted uses of the exfoliated BNNs.

3. Polymer/BNNs Nanocomposites

A major use of BNNs is in polymeric nanocomposites for thermal transport properties and others that take advantage of

the mechanical and chemically stable characteristics. The focus here is on the former,^[7,13–25,33,95,102,112,133,135–138,142–266] and those who are interested in the latter are referred to other reviews.^[19,23,26,267–270]

As nanoscale fillers in polymeric nanocomposites, BNNs are unique for their high thermal conductivity but no electrical conductivity, particularly suitable for applications that require electrical insulation, thus beyond the reach of their carbon counterparts graphene nanosheets. The high oxidation resistance of BN is also critical to some of the applications, obviously unmatched by graphene nanosheets as well. As a result, there have been more recent investigations on the development of thermally conductive polymer/BNNs nanocomposites for thermal management and related uses.^[7,13–25,33,95,102,112,133,135–138,142–266]

3.1. Representative Efforts/Results

The development effort on polymer/BNNs nanocomposites has mostly been for the higher thermal conductive performance of the nanocomposites, with emphases on the exfoliation processing to produce high-quality BNNs and/or the fabrication of the nanocomposites.^[33,112,133]

In the early study by Wang, *et al.*,^[7] BNNs obtained from relatively simple exfoliation processing of h-BN in isopropanol with vigorous sonication were dispersed into poly(vinyl alcohol) (PVA) and epoxy resin for PVA/BNNs and epoxy/BNNs nanocomposite films. The experimentally measured in-plane thermal diffusivity (TD) values of the nanocomposite films were found to increase monotonically with the increasing BNNs loading, reaching 19 mm²/s in the epoxy/BNNs film with 50 vol% BNNs. The experiments also confirmed the dependence of TD on the alignment of the embedded BNNs in the polymeric nanocomposites, with the in-plane TD of the PVA/BNNs films exhibiting up to 5-fold increases after the films were mechanically stretched, with the TD values reaching as high as 4.5 mm²/s and 8.5 mm²/s for the BNNs loadings of 10 vol% and 15 vol%, respectively.^[7] Those results were used as targets or benchmarks for further improvements in subsequent development efforts and related investigations on the production and use of BNNs in better quality, as well as in the exploration of various fabrication approaches for the nanocomposites. Since BNNs are generally considered as 2D nanomaterials, the reported studies have mostly been focusing on nanocomposite thin films and their in-plane thermal transport properties.

There has been a hypothesis that the structural defects and functional groups induced in the exfoliation processing of BNNs could actually be positive to their uses as fillers in polymeric nanocomposites, with potentially their improved dispersion and matching with the polymer matrices to result in a reduction in thermal resistance at the polymer-BNNs interface. For example, there were comparisons on the use of BNNs obtained by simple sonication in DMF *versus* BNNs from the sonication in chlorosulfonic acid (CSA) for their observed poor and good solvent dispersibility, respectively.^[95,135] The former were mixed with cellulose nanofiber for the fabrication of thermally conductive films, though in the films the dispersion of BNNs

was found to be poor, which was considered as being responsible for the relatively low observed thermal conductivity (TC) values.^[135] The latter, with their good dispersibility, were mixed well with poly(methyl methacrylate) and polybutylene terephthalate polymers for nanocomposites of higher thermal conductive performance.^[95]

Ball-milling has been a popular exfoliation method, yielding BNNs often found to be more defective, which may have both positive and negative effects on the derived polymeric nanocomposites for thermal transport applications. For example, BNNs obtained from ball-milling in aqueous sodium cholate solution were mixed with PVA polymer for the fabrication of nanocomposite papers via vacuum-filtration, but the observed TC values were rather low, about 7 W/mK even at the high BNNs loading of 94 wt%.^[136] However, better performances were found in other studies by polymeric nanocomposites derived from similarly produced BNNs.^[33] BNNs from ball-milling exfoliation were assembled into an aerogel and infiltrated with epoxy resin for nanocomposites of an organized 3D conductive network, achieving a reasonably good TC value of ~6 W/mK at 15 vol% BNNs loading.^[137]

The BNNs produced by ball-milling in aqueous urea solution are often considered as “functionalized BNNs”, probably for the improved stability of their aqueous dispersion. Such BNNs were composited with cellulose nanofibers for thin films of relatively high in-plane TC values, up to 30 W/mK in the film of 30 microns in thickness containing 70 wt% BNNs (Figure 7).^[138] Similarly, polydopamine was used as a dispersion/coating (functionalization) agent in the “one-pot” ball-milling exfoliation, and the resulting BNNs were combined with cellulose nanocrystal for nanocomposites of TC values up to 40 W/mK at the BNNs loading of 94 wt%.^[102]

The debate on the good and/or bad of defects in BNNs, as associated with the various exfoliation approaches, is obviously interesting and consequential, presenting the research community a challenging and time-consuming task for systematic evaluations. One relevant effort, though still limited, was on the comparison among BNNs from different exfoliation methods as correlated with the thermal transport performances of their derived polymeric nanocomposites, more specifically PVA/BNNs nanocomposite films.^[33] In addition to the ball-milling in urea, the other two exfoliation methods selected for comparison were the vigorous sonication in isopropanol (IPA) and the hydrothermal processing in aqueous ammonia following the treatment of sonication in IPA (designated as method-C).^[33] The BNNs obtained from the ball-milling were smaller pieces and more defective, and their corresponding polymeric nanocomposite films exhibited relatively lower TD values. On the other hand, the BNNs from method-C were apparently more favorable to their uses in thermally conductive polymeric nanocomposites, with the observed high TD values of 6 mm²/s and 6.8 mm²/s for BNNs loadings of 10 vol% and 20 vol%, respectively,^[33] thus easily topping the benchmarks achieved in the early study discussed above.^[7]

Epoxy resins are often among the choices of matrices for nanocomposites in thermal management applications.^[139–141] Similarly useful are other commodity polymers as matrices,

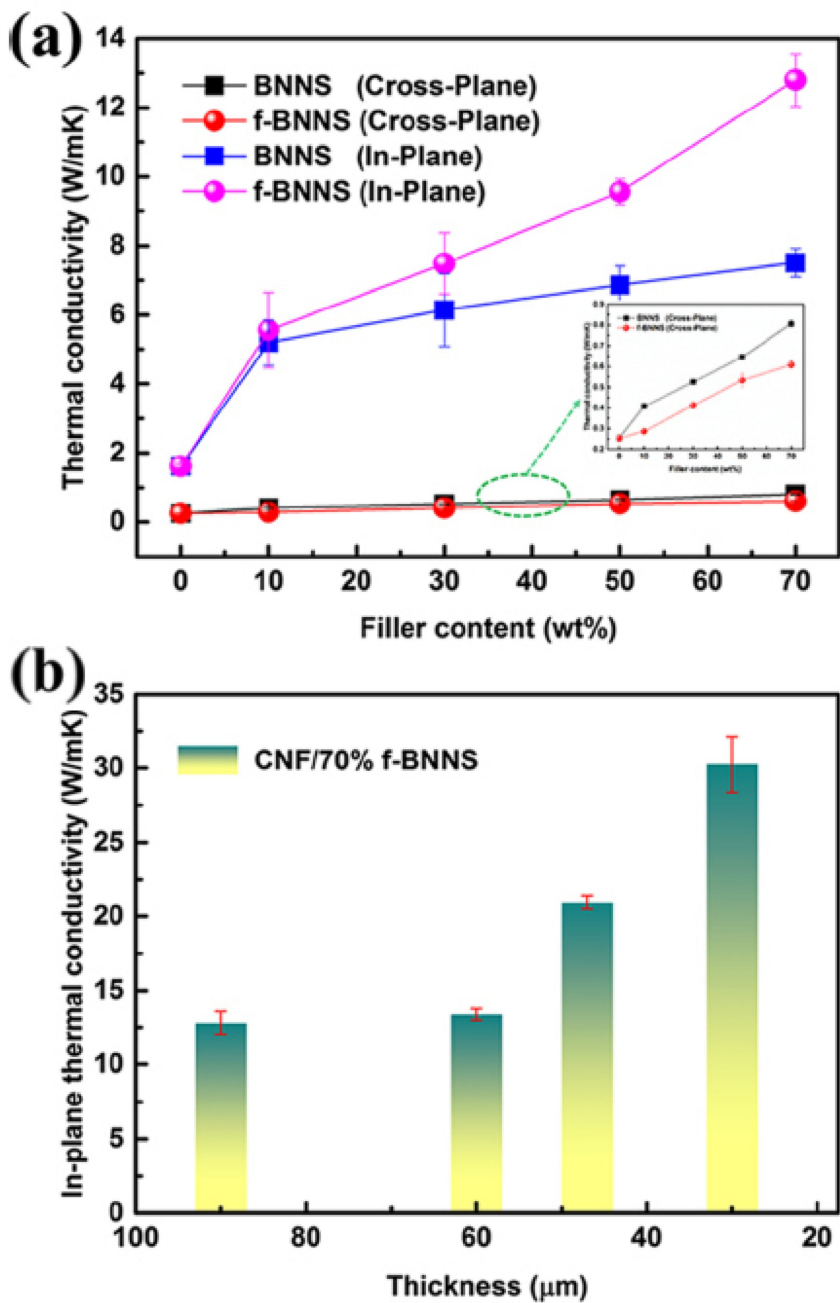


Figure 7. (a) In-plane and cross-plane TC plots for CNF/BNNs composite films prepared with BNNs obtained from sonication in DMF and then ball-milling in urea-water; (b) In-plane TC values of CNF/BNNs (70 wt%) films in different thicknesses. “Reproduced/Adapted with permission from Ref. [138]. Copyright (2017) American Chemical Society”.

including polystyrene, polyethylene, polyurethane, and others. For example, the BNNs obtained from the method-C discussed above were dispersed into polyethylene (PE) polymers for nanocomposite films, achieving a superior thermal transport performance (Figure 8). For the PE/BNNs films of 40 wt% BNNs loading, the in-plane TD was determined to be 18 mm²/s.^[142] Also interesting was the finding that the crosslinking in the films with a UV responsive crosslinking agent could augment the TD values by 20% or more, which was rationalized as being due to the crosslinking-induced structural changes in the

nanocomposite films.^[142] However, the mechanistic details on such changes that could enhance the thermal transport performance remain to be explored and understood. For other commodity polymers, there was a study in which BNNs were dispersed into styrene–ethylene–butylene–styrene copolymer and thermoplastic polyurethane for nanocomposite films with TC values of 45 W/mK and 50 W/mK, respectively.^[143,144]

Besides the issue of defects in BNNs and their related dispersion characteristics, more generally what constitute the more desirable properties of BNNs for their derived polymeric

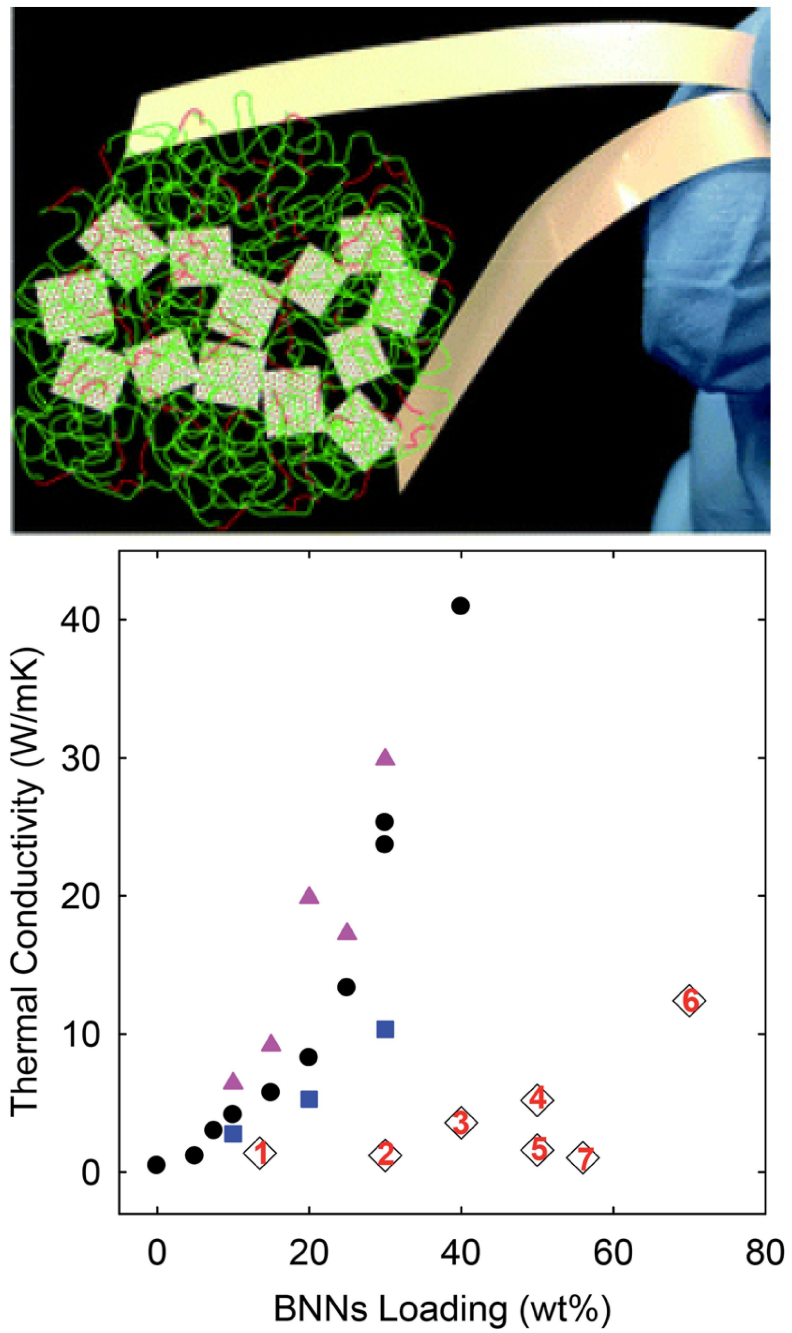


Figure 8. Top: Photos of PE/BNNs (A) and crosslinked PE/BNNs (B) films, with the cartoon illustrating the homogeneous dispersion of BNNs in PE polymers. Bottom: TC versus BNNs loading plots for PE/h-BN (square), PE/BNNs (circle), and crosslinked PE/BNNs (triangle) films compared with the results of similar films reported in the literature (1: [248]; 2: [261]; 3: [262]; 4: [263]; 5: [264]; 6: [265]; 7: [266]). "Reproduced/Adapted with permission from Ref. [142]. Copyright (2020) The Royal Society of Chemistry".

nanocomposites to achieve high thermal transport performance is yet to be established experimentally. Intuitively, a popular view has been that high-quality BNNs should be those of fewer layers and larger aspect ratios, consistent with the theoretical rationale on the longer phonon mean free paths and reduced phonon scattering, and accordingly, there have been efforts on the preparation and use of such BNNs for more thermally conductive polymeric nanocomposites.^[33,112,133] For example, it

was reported recently that BNNs of a large aspect ratio could be produced by using microfluidization technique in an ethanol-water mixture as the carrier solvent coupled with the use of appropriate pressure fluid jet (Figure 9).^[112] The dispersion of such BNNs into PVA polymer yielded more thermally conductive nanocomposite films, with the observed in-plane TC values up to ~68 W/mK at the BNNs loading of 83 wt%.

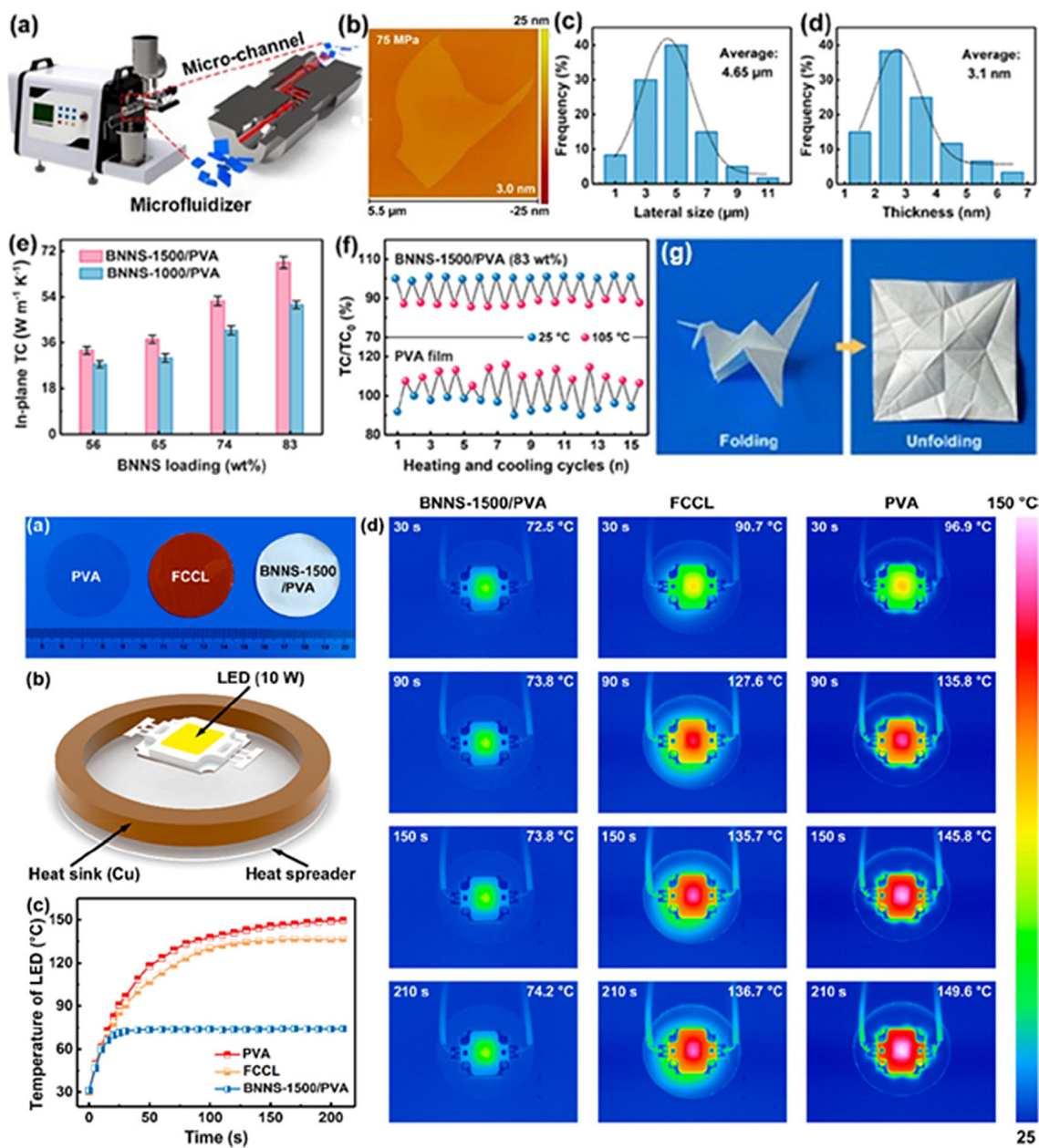


Figure 9. Top: (a) The microfluidization setup and process used for the exfoliation of h-BN for BNNs. (b) AFM image of a single BN nanosheet obtained in the microfluidization processing with the applied pressures of 75 MPa, and (c) lateral size and (d) thickness distributions of the BNNs from the same processing conditions. (e) In-plane TC values of the PVA/BNNs composite films *versus* aspect ratios and loadings of the BNNs. (f) Results of cyclic heating and cooling tests. (g) Origami foldability of the composite film with 83 wt% BNNs. Bottom: (a) Photos of neat PVA, FCCL, and PVA/BNNs composite films as heat spreaders. (b) The setup for testing the heat dissipation of high-power LED modules. (c) The central temperature evolution in the LED chip as a function of running time using various heat spreaders, and (d) the corresponding IR images. “Reproduced/Adapted with permission from Ref. [112]. Copyright (2021) American Chemical Society”.

Similarly larger aspect ratio BNNs were prepared by the exfoliation processing in supercritical fluids (SCFs).^[133] The dispersion of such BNNs into PVA polymer matrix resulted in polymeric nanocomposite films in which according to electron microscopy results the nanosheets were well-distributed and aligned, a possible advantageous consequence of the nanosheets being thinner in thickness and/or larger in lateral dimension. The observed TD values of the films were monotonically higher at higher BNNs loadings, and the performance was

at the upper end of the levels attained by similarly fabricated PVA and other polymer nanocomposite films with BNNs from various other exfoliation methods.^[137,138,145-151]

There have also been efforts on enhancing the in-plane thermal transport performance of polymer/BNNs nanocomposite films.^[148,152,153] For example, BNNs in polyvinylidene fluoride (PVDF), PVA, and epoxy resin were aligned via electrospinning fabrication, vertical folding, and post-fabrication hot-pressing, resulting in clearly observable increases in TC values.^[152] In a

layer-by-layer fabrication of PVA/BNNs nanocomposite films, the processing that combined the electrospinning of PVA fibers and the electrostatic spraying of BNNs was applied, with the observed in-plane TC value of 21 W/mK for the film of 33 wt% BNNs loading.^[153] Epoxy/BNNs nanocomposite films were also prepared by the self-assembly of BNNs on a 3D cellulose fiber structure, including sol-gel and freeze-drying processing steps and the subsequent epoxy impregnation, though the observed TC values for the films were relatively low.^[148]

The results highlighted above and obtained in many other studies, some of which are summarized in Table 2, have collectively established that the dispersion or incorporation of BNNs into polymer matrices represents an excellent approach for substantially higher TD/TC values than those of the neat matrix polymers, with the resulting nanocomposites still electronically insulating. These generally light-weight nanocomposite materials are highly valuable to many technological applications, from electronic packaging in microelectronics to thermal management in space. On the much desired performance enhancement, however, the progress has generally been slow since the previous account in 2015,^[7] with overall the achieved thermal transport performance levels still significantly below those of the comparable nanocomposites of the same polymers with graphene nanosheets as fillers. The narrowing

and closing of such a performance gap represent both major challenges and great opportunities.

3.2. Measurements and Technical Issues

In the development of thermally conductive polymer/BNNs nanocomposites, a challenge increasingly recognized in the community is with the experimental techniques to accurately determine the TD/TC values of the nanocomposites. Summarized in Table 2 are some commonly employed measurement methods in recent studies reported in the literature.

Except for a few noted ones in Table 2, the experimentally measured thermal transport parameters of the polymeric nanocomposites are mostly thermal diffusivity (TD) values, which can be converted to thermal conductivity (TC) values by using measured or estimated densities (ρ) and heat capacities (C_p) of the materials under consideration.^[271,272]

$$TC = \rho \cdot C_p \cdot TD \quad (1)$$

As summarized in Table 2, most experimental TD values of the BNNs-based nanocomposites were measured on NETZSCH LFA-447 NanoFlash and LFA-467 HyperFlash instruments,^[274]

Table 2. In-plane TD/TC Values by Various Measurement Methods for Polymeric Nanocomposite Films with BNNs from Different Exfoliation Methods/Conditions.

Polymer ^[a]	Exfoliation Method/Conditions ^[b]	BNNs Loading	TC ^[c] (W/mK)	Method ^[d]	Ref.
PVA	IPA/24 h reflux & 48 h SN @50 °C	10 vol %	4.4	LaserPIT	[33]
	IPA/24 h reflux & 48 h SN @50 °C	20 vol %	12	LaserPIT	[33]
	Urea/20 h ball-mill & 24 h SN	10 vol %	2.2	LaserPIT	[33]
	Urea/20 h ball-mill & 24 h SN	20 vol %	8.2	LaserPIT	[33]
	Ammonia-Water-IPA/3 h @260 °C	10 vol %	14	LaserPIT	[33]
	Ammonia-Water-IPA/3 h @260 °C	20 vol %	16	LaserPIT	[33]
	Ethanol-Water/20 min @400 °C	40 vol %	26	LaserPIT	[133]
	Aqueous cholate/12 h ball-mill	94 wt%	6.9	LFA-447	[136]
	IPA-Water (1:1)/4 h SN	33 wt%	21.4	LFA-467	[153]
	Urea/20 h ball-mill	90 wt%	120 ^[e]	Steady-State	[156]
PE	Ammonia-Water-IPA/48 h SN	40 wt%	41	LaserPIT	[142]
PVDF	IPA-Water/4 h SN	33 wt%	16.3	LFA-467	[152]
TPU	DMF/48 h SN	10 wt%	14.7	LFA-447	[154]
PMMA	TPU-DMF/24 h ball-mill	95 wt%	50.3	LFA-447	[143]
PBT	Chlorosulfonic acid/8 h SN	80 wt%	14.7	TA3	[95]
Epoxy	Chlorosulfonic acid/8 h SN	80 wt%	15.1	TA3	[95]
SEBS	IPA-Water/24 h ball-mill/1 h SN	15 vol %	6.1	Hot Disk	[137]
CNF	SEBS-THF/24 h ball-mill	95 wt%	45	LFA-447	[144]
	Water/8 h SN	25 wt%	22.7	LFA-467	[157]
	DMF/10 h SN & Aqueous urea 16 h ball mill	60 wt%	24	LFA-467	[135]
	DMF/10 h SN & Aqueous urea/16 h ball mill	70 wt%	30.2	LFA-467	[138]
	Dopamine/Buffer/24 h ball-mill	94 wt%	40	LFA-447	[102]
	Ethanol-Water/48 h SN	10 wt%	11.3 ^[e]	Steady-State	[158]
	IPA/48 h SN	50 wt%	145.7 ^[e]	Steady-State	[155]
CNR	Polyrhodanine/15 min roll mill with CNR	77 wt%	45.7	LFA-447	[159]
PA66	PA/15 min plasma with mechanochemistry	20 wt%	26.1	Hot Disk	[160]
PDA	Urea/20 h ball-mill	90 wt%	200 ^[e]	Steady-State	[161]

^[a] PVA: Poly(vinyl alcohol); PE: Polyethylene; PVDF: Polyvinylidene fluoride; TPU: Polyurethane; PMMA: poly(methyl methacrylate); PBT: Polybutylene terephthalate; SEBS: Styrene-ethylene-butylene-styrene; CNF: Cellulose nanofiber; CNR: Carboxylated nitrile rubber; PA66: Polyamide 66; PDA: Poly(diallyl dimethyl ammonium chloride). ^[b] IPA: Isopropanol; SN: Sonication. ^[c] Except for those noted, TD was measured for the calculation of TC based on Eq. 1. ^[d] LaserPIT [273]: Designed specifically for in-plane TD; LFA-447 and LFA-467 [274]: Based on laser flash method; Steady-State [275]: Measuring the temperature difference due to steady-state heat; TA3 [276]: Thermo-wave analysis with periodic laser heating; Hot Disk [277]: A metal disk as heat source and for sensing.

^[e] TC measured directly.

which according to the schematic and description for the instruments on the company website are based on the principle and design that “the light beam heats the lower sample surface and an IR detector measures the temperature increase on the upper sample surface”.^[274] For sample specimen of anisotropic thermal transport characteristics, such as thin polymeric nanocomposite films with BNNs or graphene nanosheets as fillers, there could be an order-of-magnitude difference between in-plane and cross-plane thermal diffusivities, as found in some of the published studies.^[102,143,144,152,153,157] By looking at the design principle,^[274] one may argue that these instruments are intrinsically more suitable for measurements in the cross-plane configuration. There are apparently software fixes that would enable the measurement of in-plane thermal diffusivities of thin film specimens, but subject to significant limitations that are associated with or depend on how thermally conductive of the film specimen being measured. There should hopefully be systematic evaluations on the capabilities and limitations with respect to the accuracy of the in-plane TD values from these instruments by using thin film standards of known thermal diffusivities over a broad range that covers the typical and targeted thermal diffusivities of polymer/BNNs nanocomposite films.

The Ulvac LaserPIT instrument based on the modified Angstrom’s method is designed specifically for measuring in-plane TD values of thin films (Table 2),^[273] not applicable to cross-plane measurements at all. Consequently, the film specimen must be thin, less than 100 nm or preferably 20–40 nm in thickness, in order to emphasize in-plane (2D) thermal diffusion. The instrument can be and has been calibrated by using the manufacturer supplied thin plates of the materials whose TD values are well established, including silver at the upper end, with the calibrations performed before, during, and after measurements of unknown samples. The pairing of this or similar instruments designed specifically for in-plane TD measurements with the NETZSCH instruments discussed above or the like that are more suitable for cross-plane TD measurements would be ideal for more accurate evaluations on the thermal transport performance of BNNs-based nanocomposites, including the necessary calibrations with known standards and the cross-checking of the TD/TC results reported in the literature.

The same calibrations with known standards and cross-checking are obviously more critical for the steady-state method, so as to further validate the apparently considerably higher TC values obtained by that method (Table 2). The concentration of extraordinarily high values from measurements by one method does not necessarily suggest errors, but does warrant extra precautions and more rigorous calibration effort.

4. Theories and Simulations

Optimizing the thermal properties of BNNs-based nanocomposites faces the challenge of navigating the high-dimensional design space spanned by parameters including filler size and shape, defect density in fillers, filler loading and dispersion,

orientational ordering of fillers, etc. Theories and simulations that predict a composite’s thermal properties from its composition and structure can help accelerate the desired optimization, as pursued in some recent studies.^[230,258,278–281]

A widely used theory for thermal nanocomposites is the effective medium theory by Nan *et al.*, which achieves a good balance between complexity and fidelity.^[278] It considers the heat conduction in fillers, in matrix, and across filler-matrix interfaces. Taking BNNs as flakes with a lateral size a_1 and thickness a_3 ($a_3 < a_1$), their composite’s effective thermal conductivities in the directions parallel to and normal to the flakes (k_{11}^* and k_{33}^* , respectively) are given by

$$\begin{aligned} k_{11}^* &= k_m \\ \frac{2 + f[\beta_{11}(1 - L_{11})(1 + \langle \cos^2 \theta \rangle) + \beta_{33}(1 - L_{33})(1 - \langle \cos^2 \theta \rangle)]}{2 - f[\beta_{11}L_{11}(1 + \langle \cos^2 \theta \rangle) + \beta_{33}L_{33}(1 - \langle \cos^2 \theta \rangle)]} & \quad (2a) \\ k_{33}^* &= \\ \frac{k_m[1 + f[\beta_{11}(1 - L_{11})(1 - \langle \cos^2 \theta \rangle) + \beta_{33}(1 - L_{33})\langle \cos^2 \theta \rangle]]}{1 - f[\beta_{11}L_{11}(1 - \langle \cos^2 \theta \rangle) + \beta_{33}L_{33}\langle \cos^2 \theta \rangle]} & \quad (2b) \end{aligned}$$

where k_p and k_m are the thermal conductivity of BNNs and the matrix, respectively. f is the volume fraction of BNNs fillers. $\langle \cos^2 \theta \rangle$ characterizes the average filler orientation. L_{11} and L_{33} are BNNs’ shape factors defined using its aspect ratio p ($p = a_3/a_1$),

$$L_{11} = L_{22} = \frac{p^2}{2(p^2 - 1)} + \frac{p}{2(1 - p^2)^{\frac{3}{2}}} \cdot \cos^{-1} p \quad (3a)$$

$$L_{33} = 1 - 2L_{11} \quad (3b)$$

$$\beta_{ii} = \frac{k_{ii}^c - k_m}{k_m + L_{ii}(k_{ii}^c - k_m)} \quad (i = 1 \text{ and } 2) \quad (3c)$$

$$k_{ii}^c = \frac{k_p}{1 + \gamma L_{ii} k_p / k_m} \quad (3d)$$

$$\gamma = (1 + 2p) \frac{k_m}{G a_3} \quad (3e)$$

where G is the thermal conductance at the filler-matrix interfaces.

At a given BNNs filler loading, the above theory predicts that the conductivity of a composite is enhanced as BNNs’ size and aspect ratio increase, BNNs becomes more aligned, or the thermal conductance at BNNs-matrix interfaces increases. In practice, not all these parameters can be enhanced simultaneously, and the theory provides insights into what tradeoff and compromise can be leveraged. In this regard, insights from graphene composite optimization based on this theory may be helpful for the development of BNNs composites. For example, while introducing defects or functionalization to graphene generally reduces its intrinsic thermal conductivity, doing so helps increase the thermal conductance at graphene-matrix interfaces.^[279,280] The above theory, when applied to graphene composites, predicts that, for small graphene flakes, introducing

defects into them can enhance the conductivity of their composites,^[279] namely the compromise in favor of the improved thermal conductance at graphene-matrix interfaces.

A limitation of the above theory and its numerous extensions is that material parameters including filler's thermal conductivity and interfacial thermal conductance, which depend on the molecular details of the filler and matrices, must be provided as input. This limitation can be addressed using molecular simulations, which can explicitly resolve the BNNs, matrices, and their interfaces. While molecular simulations of BNNs composites are quite limited, insightful studies, especially those featuring BNNs and epoxy polymers, have been reported.^[230,258,281]

Liu, *et al.* analyzed the thermal and rheological properties of epoxy/BNNs composites.^[230] Using molecular dynamics simulations, they investigated how BNNs enhance the TC performance by modeling the interactions between the epoxy resin and curing agent, epoxy and BNNs, and also interactions within BNNs using CVFF, Lennard-Jones, and Tersoff potentials, respectively. They demonstrated the validity of their model by comparing the predicted values of thermal and rheological properties, such as glass transition temperature (T_g), coefficient of thermal expansion (CTE), TC and viscosity (η), for the epoxy resin with previously reported experimental data as well as those from MD simulations. However, the TC values of epoxy/BNNs composites at various BNNs loadings predicted by their simulation did not agree well with the reported experimental values, probably due to the use in their model of thermally disconnected randomly distributed BNNs, which is far from the structures in highly oriented epoxy/BNNs composites for the reported TC values.

Li, *et al.* used molecular dynamics simulations to investigate the influence of interfaces in epoxy resin filled with pristine as well as surface functionalized BNNs as nanofillers.^[281] They used the radial distribution density (RDD) and interfacial binding energy (IBE), and found that the physical and chemical properties near an interface were significantly different from the regions far from it. In addition, the interface compatibility and molecular chain mobility (MCM) in epoxy/BNNs nanocomposites with BNNs of different functionalized surfaces were analyzed by using cohesive energy density (CED), free volume fraction (FFV), and radial mean square displacement (RMSD). They classified interfaces into three regions: i) compact region (mass density 15~25% higher than that of the normal region, with significantly small chain mobility), ii) buffer region, and iii) normal region (mass density ~1.12 g/cm³ and chain mobility similar to epoxy resin). Moreover, the interfacial interaction strength and compatibility were found to increase with the functional density of BNNs functionalized by CH₃-(CH₂)₄-O-radicals. The results illustrated the interfacial characteristics of nanocomposites from the atomic level and the multi-layer approach, making the modeling approach potentially applicable to the understanding of the thermal transport in the nanocomposites. However, more desirable would be comparisons of the modeling results with available experimental data.

Zhu, *et al.* presented a more comprehensive molecular dynamics (MD) simulation study on the influence of BN nano-

fillers on properties of epoxy using the Accelrys Materials Studio 8.0 software.^[258] The modeling was on the interaction between molecules based on the universal force field (UFF), and the system was optimized by repeating twice the process of relaxations within a series of constant-volume (NVT), constant-pressure (NPT), and again NVT ensembles for an un-crosslinked model. The TC values were calculated by using the reverse non-equilibrium molecular dynamics (RNEMD) method, yielding 0.18 W/mK for the neat epoxy in comparison with the experimental value of 0.2 W/mK. Also investigated in the modeling were the effects of the nanofiller shapes, including nanoparticle, nanotube, and nanosheet, volume fractions, and aspect ratios on the thermal transport properties. The results from the RNEMD simulation and Nielsen's theoretical model suggested the ranking in the effectiveness of different BN nanofillers as nanosheet better than nanotubes and better than nanoparticles. The temperature gradient distribution and phonon density of states (PDOS) were analyzed to elucidate the heat-conducting mechanism in the epoxy composites. Building upon the broad selection of BN nanofillers and modeling techniques in the reported study, further investigations might benefit from expanded models that include the effect of relative nanofiller orientations and connections in the composite matrix.

The polymer/BNNs nanocomposites are complicated systems with many parameters, presenting intrinsically challenging tasks for theories and simulations. Nevertheless, modeling efforts like those highlighted here and others offer valuable insights into the structures and properties of the nanocomposites, especially for those parameters that are difficult or even impossible to probe experimentally.

5. Summary and Perspectives

There have been steadily increasing numbers of investigations on the exfoliation of h-BN into BNNs, which suggest the growing recognition that BNNs offer some unique properties and applications not available to or unmatched by their more popular carbon counterparts graphene nanosheets. Recent studies have also reminded the relevant research community on the major challenges and related opportunities in the development of new and more effective exfoliation approaches for high-quality BNNs, especially on the needs for novel processing methods and conditions, convenient and consistent parameters and qualifications for the quick assessment of the exfoliation outcomes, and reliable correlations of the exfoliation and the quality of thus produced BNNs with the performance benchmarks in specific applications such as the TD/TC values of the corresponding polymer/BNNs nanocomposites, which may also be guided by theoretical and modeling efforts.

For the exfoliation that emphasizes the 2D characteristics of BNNs in reference to graphene nanosheets, the favorable processing conditions seem to be those that are sufficiently harsh to be able to overcome the stronger inter-layer binding-like interactions in h-BN, but still gentle enough not to break the h-BN into tiny pieces. The seemingly contradictory com-

promise may be achieved with the aid of some specific functionalization agents or special solvent properties such as those found in supercritical fluids (SCFs) and mixtures. The commonly stated objective of exfoliation efforts in reported investigations is for "high-quality BNNs", though the definition on the high quality appears somewhat subjective, which may ultimately depend on how and where the BNNs are used and for what purposes. It must also be stressed here that the real issues and challenges for further investigations may not be the development of "more effective exfoliation approaches and methods" for "higher-quality" BNNs, but more importantly the understanding and agreement on their definitions and the related experimental consequences. There is a critical need for the establishment of broadly agreed and experimentally validated criteria for the specific structural and morphological parameters of exfoliation produced BNNs that constitute the targeted high quality, which may also be defined differently for different end uses of the BNNs. These will naturally lead to the establishment of the related parameters that define the aim and effectiveness (and also efficiency) of the desired exfoliation approaches and methods.

There has been a natural tendency in the research community to couple the exfoliation preparation of BNNs and the performance of their derived thermally conductive nanocomposite materials. Such mindset and practice might make sense practically in terms of being able to get to the targeted nanocomposites without knowing much about the detailed relationships between the structural and morphological parameters of both the BNNs and the corresponding nanocomposites, but the lack of understandings on such details may hinder the development of nanocomposite materials with truly breakthrough thermal transport performances. In fact, it may be necessary to separate the consideration of the exfoliation preparation of BNNs from that of their derived nanocomposites, namely to establish the independent criteria and definitions discussed above for the exfoliation and produced BNNs, because the performance of the nanocomposites is subject to many other effects such as the fabrication methods and conditions, TC/TD measurement techniques and limitations, and various other complications. The separated considerations will enable more informative and meaningful correlations between the well-defined quality parameters of BNNs and the performance of the corresponding nanocomposites for improvements in the two independently and then further correlations to continue the cycle toward optimization.

For BNNs as thermally conductive nanofillers in polymeric nanocomposites, to achieve the goal of ultimately having the thermal transport performance of the nanocomposites match the performance of those with graphene nanosheets as nanofillers may prove more than challenging, or more like an inspiration only as some might argue. Nevertheless, one may also argue that the comparison and performance matching between polymeric nanocomposites with BNNs and their carbon counterparts as nanofillers may be missing the point, as in fact there should be more opportunities in leveraging the many superior properties of BNNs, especially their extreme stabilities in addition to being electronically insulating. In short,

BNNs have a bright future, and their related development efforts will prove very rewarding.

Acknowledgments

Financial support from NASA (80NSSC18M0033) is gratefully acknowledged. J.L.Q. was a participant of Palmetto Academy, a summer undergraduate research program of the South Carolina Space Grant Consortium.

Conflict of Interest

The authors declare no conflict of interest.

Keywords: boron nitride • exfoliation • nanosheets • polymeric nanocomposites • thermal conductivity

- [1] T. Ishii, T. Sato, Y. Sekikawa, M. Iwata, *J. Cryst. Growth* **1981**, *52*, 285–289.
- [2] R. Pease, *Nature* **1950**, *165*, 722–723.
- [3] R. T. Paine, C. K. Narula, *Chem. Rev.* **1990**, *90*, 73–91.
- [4] D. Golberg, Y. Bando, Y. Huang, T. Terao, M. Mitome, C. Tang, C. Y. Zhi, *ACS Nano* **2010**, *4*, 2979–2993.
- [5] O. Hod, *J. Chem. Theory Comput.* **2012**, *8*, 1360–1369.
- [6] Y. Lin, J. W. Connell, *Nanoscale* **2012**, *4*, 6908–6939.
- [7] M. J. Meziani, W.-L. Song, P. Wang, F. Lu, Z. Hou, A. Anderson, H. Maimaiti, Y.-P. Sun, *ChemPhysChem* **2015**, *16*, 1339–1346.
- [8] L. H. Li, J. Cervenka, K. Watanabe, T. Taniguchi, Y. Chen, *ACS Nano* **2014**, *8*, 1457–1462.
- [9] L. H. Li, T. Xing, Y. Chen, R. Jones, *Adv. Mater. Interfaces* **2014**, *1*, 1300132.
- [10] D. Golberg, Y. Bando, K. Kurashima, T. Sato, *Scr. Mater.* **2001**, *44*, 1561–1565.
- [11] Y. Chen, J. Zou, S. J. Campbell, G. L. Caer, *Appl. Phys. Lett.* **2004**, *84*, 2430–2432.
- [12] G. E. Spriggs in *Group VIII Advanced Materials and Technologies: Powder Metallurgy Data, Refractory, Hard and Intermetallic Materials*, Vol. 2 A2 (Eds.: R. Ruthardt, H. W. Landolt-Börnstein), Springer, Berlin, **2002**, pp. 118–139.
- [13] W.-L. Song, P. Wang, L. Cao, A. Anderson, M. J. Meziani, A. J. Farr, Y.-P. Sun, *Angew. Chem. Int. Ed.* **2012**, *51*, 6498–6501; *Angew. Chem.* **2012**, *124*, 6604–6607.
- [14] W. Meng, Y. Huang, Y. Q. Fu, Z. Wang, C. Zhi, *J. Mater. Chem. C* **2014**, *2*, 10049–10061.
- [15] J. Yin, J. Li, Y. Hang, J. Yu, G. Tai, X. Li, Z. Zhang, W. Guo, *Small* **2016**, *12*, 2942–2968.
- [16] G. R. Bhimanapati, N. R. Glavin, J. A. Robinson in *2D Boron Nitride: Synthesis and Applications in 2D Materials* (Eds.: F. Iacopi, J. J. Boeckl, C. Jagadish), Elsevier Science & Technology, Amsterdam, **2016**, pp. 101–148.
- [17] W. Luo, Y. Wang, E. Hitz, Y. Lin, B. Yang, L. Hu, *Adv. Funct. Mater.* **2017**, *27*, 1701450.
- [18] C. Yu, J. Zhang, W. Tian, X. Fan, Y. Yao, *RSC Adv.* **2018**, *8*, 21948–21967.
- [19] V. Guerra, C. Wan, T. McNally, *Prog. Mater. Sci.* **2019**, *100*, 170–186.
- [20] X. Shen, J. K. Kim, *Funct. Compos. Struct.* **2020**, *2*, 022001.
- [21] Y. Guo, K. Ruan, X. Shi, X. Yang, J. Gu, *Compos. Sci. Technol.* **2020**, *193*, 108134.
- [22] D. M. Lima, A. C. Chinellato, M. Champeau, *Soft Matter* **2021**, *17*, 4475–4488.
- [23] M. G. Rasul, A. Kiziltas, B. Arfaei, B. R. Shahbazian-Yassar, *NPJ 2D Mater. Appl.* **2021**, *5*, 56.
- [24] Y. Zhang, J. Ma, N. Wei, J. Yang, Q.-X. Pei, *Phys. Chem. Chem. Phys.* **2021**, *23*, 753–776.
- [25] J. Wang, L. Zhang, L. Wang, W. Lei, Z.-S. Wu, *Energy Environ. Mater.* **2021**, *0*, 1–35.

- [26] K. Zhang, Y. Feng, F. Wang, Z. Yang, J. Wang, *J. Mater. Chem. C* **2017**, *5*, 11992–12022.
- [27] H. Li, Y. Li, A. Aljarb, Y. Shi, L.-J. Li, *Chem. Rev.* **2018**, *118*, 6134–6150.
- [28] Q. Weng, X. Wang, X. Wang, Y. Bando, D. Golberg, *Chem. Soc. Rev.* **2016**, *45*, 3989–4012.
- [29] D. V. Shtansky, K. L. Firestein, D. V. Golberg, *Nanoscale* **2018**, *10*, 17477–17493.
- [30] Q. Cai, D. Scullion, W. Gan, A. Falin, S. Zhang, K. Watanabe, T. Taniguchi, Y. Chen, E. J. G. Santos, L. H. Li, *Sci. Adv.* **2019**, *5*, eaav0129.
- [31] Q. Cai, D. Scullion, W. Gan, A. Falin, P. Cizek, S. Liu, J. H. Edgar, R. Liu, B. C. C. Cowie, E. J. G. Santos, L. H. Li, *Phys. Rev. Lett.* **2020**, *125*, 085902.
- [32] H. Tao, Y. Zhang, Y. Gao, Z. Sun, C. Yan, J. Texter, *Phys. Chem. Chem. Phys.* **2017**, *19*, 921–960.
- [33] Z. D. Wang, M. J. Meziani, A. K. Patel, P. Priego, W. Wirth, P. Wang, Y.-P. Sun, *Ind. Eng. Chem. Res.* **2019**, *58*, 18644–18653.
- [34] J. N. Coleman, M. Lotya, A. O'Neill, S. D. Bergin, P. J. King, U. Khan, K. Young, A. Gaucher, S. De, R. J. Smith, I. V. Shvets, S. K. Arora, G. Stanton, H. Y. Kim, K. Lee, G. T. Kim, G. S. Duesberg, T. Hallam, J. J. Boland, J. J. Wang, J. F. Donegan, J. C. Grunlan, G. Moriarty, A. Shmeliov, R. J. Nicholls, J. M. Perkins, E. M. Grieveson, K. Theuwissen, D. W. McComb, P. D. Nellist, V. Nicolosi, *Science* **2011**, *331*, 568–571.
- [35] C. Zhi, Y. Bando, C. Tang, H. Kuwahara, D. Golberg, *Adv. Mater.* **2009**, *21*, 2889–2893.
- [36] J. H. Warner, M. H. Rümmeli, A. Bachmatiuk, B. Büchner, *ACS Nano* **2010**, *4*, 1299–1304.
- [37] J. Shen, Y. He, J. Wu, C. Gao, K. Keyshar, X. Zhang, Y. Yang, M. Ye, R. Vajtai, J. Lou, P. Ajayan, *Nano Lett.* **2015**, *15*, 5449–5454.
- [38] K. R. Paton, V. Eswaraiah, B. Claudia, J. S. Ronan, K. Umar, O. N. Arlene, B. Conor, L. Mustafa, M. I. Oana, K. Paul, H. Tom, B. Sebastian, M. Peter, P. Pawel, A. Iftikhar, M. Matthias, P. Henrik, L. Edmund, C. João, E. O. B. Sean, K. M. Eva, M. S. Beatriz, S. D. Georg, M. Niall, J. P. Timothy, D. Clive, C. Alison, N. Valeria, N. C. Jonathan, *Nat. Mater.* **2014**, *13*, 624–630.
- [39] G. Duan, Y. Wang, J. Yu, J. Zhu, Z. Hu, *Macromol. Mater. Eng.* **2019**, *304*, 1900310.
- [40] X. Chen, R. A. Boulos, J. F. Dobson, C. L. Raston, *Nanoscale* **2013**, *5*, 498–502.
- [41] Y. Lin, T. V. Williams, T.-B. Xu, W. Cao, H. E. Elsayed-Ali, J. W. Connell, *J. Phys. Chem. C* **2011**, *115*, 2679–2685.
- [42] D. Kim, S. Nakajima, T. Sawada, M. Iwasaki, S. Kawauchi, C. Zhi, Y. Bando, D. Golberg, T. Serizawa, *Chem. Commun.* **2015**, *51*, 7104–7107.
- [43] J. Kim, S. Kwon, D.-H. Cho, B. Kang, H. Kwon, Y. Kim, S. O. Park, G. Y. Jung, E. Shin, W.-G. Kim, H. Lee, G. H. Ryu, M. Choi, T. H. Kim, J. Oh, S. Park, S. K. Kwak, S. W. Yoon, D. Byun, Z. Lee, C. Lee, *Nat. Commun.* **2015**, *6*, 8294.
- [44] K.-G. Zhou, N.-N. Mao, H.-X. Wang, Y. Peng, H.-L. Zhang, *Angew. Chem. Int. Ed.* **2011**, *50*, 10839–10842; *Angew. Chem.* **2011**, *123*, 11031–11034.
- [45] K. L. Marsh, M. Souliman, R. B. Kaner, *Chem. Commun.* **2015**, *51*, 187–190.
- [46] U. Halim, C. R. Zheng, Y. Chen, Z. Lin, S. Jiang, R. Cheng, Y. Huang, X. Duan, *Nat. Commun.* **2013**, *4*, 2213.
- [47] T. Habib, D. S. Devarajan, F. Khabaz, D. Parviz, T. C. Achee, R. Khare, M. J. Green, *Langmuir* **2016**, *32*, 11591–11599.
- [48] S.-Y. Xie, W. Wang, K. A. S. Fernando, X. Wang, Y. Lin, Y.-P. Sun, *Chem. Commun.* **2005**, 3670–3672.
- [49] Y. Lin, T. V. Williams, J. W. Connell, *J. Phys. Chem. Lett.* **2010**, *1*, 277–283.
- [50] Y. Lin, T. V. Williams, W. Cao, H. E. Elsayed-Ali, J. W. Connell, *J. Phys. Chem. C* **2010**, *114*, 17434–17439.
- [51] A. Nag, K. Raindogia, K. P. S. S. Hembram, R. Datta, U. V. Wangmare, C. N. R. Rao, *ACS Nano* **2010**, *4*, 1539–1544.
- [52] L. Cao, S. Emami, K. Lafdi, *Mater. Express* **2014**, *4*, 165–171.
- [53] A. Anderson, Z.-L. Hou, W.-L. Song, M. J. Meziani, P. Wang, F. Lu, J. Lee, L. Xu, Y.-P. Sun, *J. Mater. Sci. Mater. Electron.* **2017**, *28*, 9048–9055.
- [54] A. Chae, S.-J. Park, B. Min, I. In, *Mater. Res. Express* **2018**, *5*, 015036.
- [55] L. Guardia, J. I. Paredes, R. Rozada, S. Villar-Rodil, A. Martínez-Alonso, J. M. D. Tascón, *RSC Adv.* **2014**, *4*, 14115–14127.
- [56] N. D. Mansukhani, L. M. Guiney, P. J. Kim, Y. Zhao, D. Alducin, A. Ponce, E. Larios, M. J. Yacaman, M. C. Hersam, *Small* **2016**, *12*, 294–300.
- [57] R. J. Smith, P. J. King, M. Lotya, C. Wirtz, U. Khan, S. De, A. O'Neill, G. S. Duesberg, J. C. Grunlan, G. Moriarty, J. Chen, J. Wang, A. I. Minett, V. Nicolosi, J. N. Coleman, *Adv. Mater.* **2011**, *23*, 3944–3948.
- [58] J. Zhu, J. Kang, J. Kang, D. Jariwala, J. D. Wood, J. W. T. Seo, K. S. Chen, T. J. Marks, M. C. Hersam, *Nano Lett.* **2015**, *15*, 7029–7036.
- [59] W. Wang, S. J. Chen, F. B. De Souza, B. Wu, W. H. Duan, *Nanoscale* **2018**, *10*, 1004–1014.
- [60] C. Backes, D. Campi, B. M. Szydlowska, K. Synnatschke, E. Ojala, F. Rashvand, A. Harvey, A. Griffin, Z. Sofer, N. Marzari, J. N. Coleman, D. D. O'Regan, *ACS Nano* **2019**, *13*, 7050–7061.
- [61] A. D. S. McWilliams, C. Martínez-Jiménez, A. M. Ya'akobi, C. J. Ginestra, Y. Talmon, M. Pasquali, A. A. Marti, *ACS Appl. Mater. Interfaces* **2021**, *4*, 142–151.
- [62] R. Bari, D. Parviz, F. Khabaz, C. D. Klaassen, S. D. Metzler, M. J. Hansen, R. Khare, M. J. Green, *Phys. Chem. Chem. Phys.* **2015**, *17*, 9383–9393.
- [63] P. May, U. Khan, J. M. Hughes, J. N. Coleman, *J. Phys. Chem. C* **2012**, *116*, 11393–11400.
- [64] T. Sainsbury, A. Satti, P. May, Z. Wang, I. McGovern, Y. K. Gun'ko, J. Coleman, *J. Am. Chem. Soc.* **2012**, *134*, 18758–18771.
- [65] A. C. M. Moraes, W. J. Hyun, J.-W. T. Seo, J. R. Downing, J.-M. Lim, M. C. Hersam, *Adv. Funct. Mater.* **2019**, *29*, 1902245.
- [66] X. Ge, W. J. Liang, J. F. Ge, X. J. Chen, J. Y. Ji, X. Y. Pang, M. He, X. M. Feng, *Materials* **2019**, *12*, 104.
- [67] A. A. Muhabieb, C. C. Cheng, J. J. Huang, Z. S. Liao, S. Y. Huang, C. W. Chiu, D. J. Lee, *Chem. Mater.* **2017**, *29*, 8513–8520.
- [68] Z. Wang, Y. Wen, S. Zhao, W. Zhang, Y. Ji, S. Zhang, J. Li, *Ind. Crops Prod.* **2019**, *137*, 239–247.
- [69] W. Yang, A. C. Y. Yuen, P. Ping, R.-C. Wei, L. Hua, Z. Zhu, A. Li, S.-E. Zhu, L.-L. Wang, J. Liang, T. B. Y. Chen, B. Yu, J.-Y. Si, H.-D. Lu, Q. N. Chan, G. H. Yeoh, *Composites Part A* **2019**, *119*, 196–205.
- [70] J. Biscarat, M. Bechelany, C. Pochat-Bohatier, P. Miele, *Nanoscale* **2015**, *7*, 613–618.
- [71] Y. Li, H. Zhu, F. Shen, J. Wan, S. Lacey, Z. Fang, H. Dai, L. Hu, *Nano Energy* **2015**, *13*, 346–354.
- [72] W. Liu, C. Zhao, R. Zhou, D. Zhou, Z. Liu, X. Lu, *Nanoscale* **2015**, *7*, 9919–9926.
- [73] Y. Ge, J. Wang, Z. Shi, J. Yin, *J. Mater. Chem.* **2012**, *22*, 17619–17624.
- [74] J. Thompson, A. Crossley, P. D. Nellist, V. Nicolosi, *J. Mater. Chem.* **2012**, *22*, 23246–23253.
- [75] X. Chen, R. A. Boulos, P. K. Eggers, C. L. Raston, *Chem. Commun.* **2012**, *48*, 11407–11409.
- [76] F. Zhang, X. Chen, R. A. Boulos, F. M. Yasin, H. Lu, C. Raston, H. Zhang, *Chem. Commun.* **2013**, *49*, 4845–4847.
- [77] R. Worsley, L. Pimpolari, D. McManus, N. Ge, R. Ionescu, J. A. Wittkopf, A. Alieva, G. Bassi, M. Macucci, G. Iannaccone, K. S. Novoselov, H. Holder, G. Fiori and C. Casiraghi, *ACS Nano* **2019**, *13*, 54–60.
- [78] H. Yang, F. Withers, E. Gebremedhn, E. Lewis, L. Britnell, A. Felten, V. Palermo, S. Haigh, D. Beljonne, C. Casiraghi, *2D Mater.* **2014**, *1*, 011012.
- [79] D. McManus, S. Vranic, F. Withers, V. Sanchez-Romaguera, M. Macucci, H. Yang, R. Sorrentino, K. Parvez, S. K. Son, G. Iannaccone, K. Kostarelos, G. Fiori, C. Casiraghi, *Nat. Nanotechnol.* **2017**, *12*, 343–350.
- [80] M. Du, Y. Wu, X. Hao, *CrystEngComm* **2013**, *15*, 1782–1786.
- [81] G. R. Bhimanapati, D. Kozuch, J. A. Robinson, *Nanoscale* **2014**, *6*, 11671–11675.
- [82] L. Jing, H. Li, R. Y. Tay, B. Sun, S. H. Tsang, O. Cometto, J. Lin, E. H. T. Teo, A. I. Y. Tok, *ACS Nano* **2017**, *11*, 3742–3751.
- [83] E. Czarniewska, L. Mrówczyńska, M. Jędrzejczak-Silicka, P. Nowicki, M. Trukawka, E. Mijowska, *Sci. Rep.* **2019**, *9*, 14027.
- [84] W. Zhang, M. M. Rahman, F. Ahmed, N. S. Lopa, C. Ge, T. Ryu, S. Yoon, L. Jin, H. Jang, W. Kim, *Nanotechnology* **2020**, *31*, 425604.
- [85] J. Ren, L. Stagi, P. Innocenzi, *J. Mater. Sci.* **2021**, *56*, 4053–4079.
- [86] W. S. Hummers, R. E. Offeman, *J. Am. Chem. Soc.* **1958**, *80*, 1339.
- [87] D. C. Marcano, D. V. Kosynkin, J. M. Berlin, A. Sinitskii, Z. Sun, A. Slesarev, L. B. Alemany, W. Lu, J. M. Tour, *ACS Nano* **2010**, *4*, 4806–4814.
- [88] X. Li, X. Hao, M. Zhao, Y. Wu, J. Yang, Y. Tian, G. Qian, *Adv. Mater.* **2013**, *25*, 2200–2204.
- [89] L. Fu, G. Lai, G. Chen, C.-T. Lin, A. Yu, *ChemistrySelect* **2016**, *1*, 1799–1803.
- [90] W. Yang, N.-N. Wang, P. Ping, A. C.-Y. Yuen, A. Li, S. E. Zhu, L. Wang, J. Wu, T. B. Y. Chen, J.-Y. Si, B.-D. Rao, H.-D. Lu, Q. N. Chan, G.-H. Yeoh, *ACS Appl. Mater. Interfaces* **2018**, *0*, 40032–40043.
- [91] W. Sun, Y. Meng, Q. Fu, F. Wang, G. Wang, W. Gao, X. Huang, F. Lu, *ACS Appl. Mater. Interfaces* **2016**, *8*, 9881–9888.
- [92] F. Yang, X. Sun, Z. Yao, *Langmuir* **2021**, *37*, 6442–6450.
- [93] Y. Wang, Z. Shi, J. Yin, *J. Mater. Chem.* **2011**, *21*, 11371–11377.
- [94] K. Jasuja, K. Ayinde, C. L. Wilson, S. K. Behura, M. A. Ikenberry, D. Moore, K. Hohn, V. Berry, *ACS Nano* **2018**, *12*, 9931–9939.
- [95] T. Morishita, H. Okamoto, *ACS Appl. Mater. Interfaces* **2016**, *8*, 27064–27073.

- [96] D. Lee, B. Lee, K. H. Park, H. J. Ryu, S. Jeon, S. H. Hong, *Nano Lett.* **2015**, *15*, 1238–1244.
- [97] O.-S. Kwon, D. Lee, S. P. Lee, Y. G. Kang, N. C. Kim, S. H. Song, *RSC Adv.* **2016**, *6*, 59970–59975.
- [98] D. Lee, S. Lee, S. Byun, K. W. Paik, S. H. Song, *Composites Part A* **2018**, *107*, 217–223.
- [99] W. Lei, V. N. Mochalin, D. Liu, S. Qin, Y. Gogotsi, Y. Chen, *Nat. Commun.* **2015**, *6*, 8849.
- [100] L. Liu, Z. Xiong, D. Hu, G. Wu, B. Liu, P. Chen, *Chem. Lett.* **2013**, *42*, 1415.
- [101] W. Lei, D. Liu, Y. Chen, *Adv. Mater. Interfaces* **2015**, *2*, 1400529.
- [102] C. Yu, Q. Zhang, J. Zhang, R. Geng, W. Tian, X. Fan, Y. Yao, *ACS Appl. Nano Mater.* **2018**, *1*, 4875–4883.
- [103] L. H. Li, Y. Chen, G. Behan, H. Zhang, M. Petracic, A. M. Glushenkov, *J. Mater. Chem.* **2011**, *21*, 11862–11866.
- [104] S. Chen, R. Xu, J. Liu, X. Zou, L. Qiu, F. Kang, B. Liu, H.-M. Cheng, *Adv. Mater.* **2019**, *31*, 1804810.
- [105] Y. Yao, Z. Lin, Z. Li, X. Song, K.-S. Moon, C.-P. Wong, *J. Mater. Chem.* **2012**, *22*, 13494–13499.
- [106] D. Fan, J. Feng, J. Liu, T. Gao, Z. Ye, M. Chen, X. Lv, *Ceram. Int.* **2016**, *42*, 7155–7163.
- [107] D. Ji, Z. Wang, Y. Zhu, H. Yu, *Ceram. Int.* **2020**, *46*, 21084–21089.
- [108] J.-H. Ding, H.-R. Zhao, H.-B. Yu, *2D Mater.* **2018**, *5*, 045015.
- [109] Y. C. Yang, Z. G. Song, G. Y. Lu, Q. H. Zhang, B. Zhang, C. Wang, X. Y. Li, L. Gu, X. M. Xie, H. J. Gao, J. Lou, *Nature* **2021**, *594*, 57–61.
- [110] A. Merlo, V. R. S. S. Mokkapati, S. Pandit, I. Mijakovic, *Biomater. Sci.* **2018**, *6*, 2298–2311.
- [111] L. Stagi, J. Ren, P. Innocenzi, *Materials* **2019**, *12*, 3905.
- [112] Q. Yan, W. Dai, J. Gao, X. Tan, L. Lv, J. Ying, X. Lu, J. Lu, Y. Yao, W. Q. Ping, R. Sun, J. Yu, N. Jiang, D. Chen, C.-P. Wong, R. Xiang, S. Maruyama, C.-T. Lin, *ACS Nano* **2021**, *15*, 6489–6498.
- [113] T. Morishita, H. Okamoto, Y. Katagiri, M. Matsushita, K. Fukumori, *Chem. Commun.* **2015**, *51*, 12068–12071.
- [114] G. Garcia, M. Atilhan, S. Aparicio, *Phys. Chem. Chem. Phys.* **2016**, *18*, 1212–1224.
- [115] X. Li, Y. Feng, C. Chen, Y. S. Ye, H. Zeng, H. Qu, J. W. Liu, X. Zhou, S. Long, X. Xie, *J. Mater. Chem. A* **2018**, *6*, 20500–20512.
- [116] Y.-P. Sun, H. W. Rollins, J. Bandara, M. J. Meziani, C. E. Bunker in *Supercritical Fluid Technology in Materials Science and Engineering: Synthesis, Properties, and Applications: Preparation and processing of nanoscale materials by supercritical fluid technology*, (Eds.: Y.-P. Sun), Marcel Dekker, New York, **2002**, pp. 491–576.
- [117] M. J. Meziani, P. Pathak, Y.-P. Sun, in *Handbook of Semiconductor Manufacturing Technology: Supercritical carbon dioxide in semiconductor cleaning*, (Eds.: R. Doering, Y. Nishi), CRC Press (Taylor & Francis Group), Boca Raton, FL, **2007**, Chapter 6.
- [118] E. Gulari, G. K. Serhatkulu, *US Patent Application 00014861A1*, **2005**.
- [119] H. Gao, G. Hu, *RSC Adv.* **2016**, *6*, 10132–10143.
- [120] S. Padmajan Sasikala, P. Poulin, C. Aymonier, *Adv. Mater.* **2016**, *28*, 2663–2691.
- [121] Y. Ren, Q. Xu, *Energy Environ. Mater.* **2018**, *1*, 46–60.
- [122] Z. Sun, Q. Fan, M. Zhang, S. Liu, H. Tao, J. Texter, *Adv. Sci. Eng. Sci.* **2019**, *6*, 1901084.
- [123] D. Rangappa, K. Sone, M. Wang, U. K. Gautam, D. Golberg, H. Itoh, M. Ichihara, I. Honma, *Chem. Eur. J.* **2010**, *16*, 6488–6494.
- [124] C. Liu, G. Hu, *Ind. Eng. Chem. Res.* **2014**, *53*, 14310–14314.
- [125] J.-H. Jang, D. Rangappa, Y.-U. Kwon, I. Honma, *J. Mater. Chem.* **2011**, *21*, 3462–3466.
- [126] A. Hadji, J. Karimi-Sabet, S. M. A. Moosavian, S. Ghorbanian, *J. Supercrit. Fluids* **2016**, *107*, 92–105.
- [127] C. Liu, G. Hu, H. Gao, *J. Supercrit. Fluids* **2012**, *63*, 99–104.
- [128] R. M. Ibarra, M. Goto, J. García-Serna, S. M. G. Montes, *Carbon Lett.* **2021**, *31*, 99–105.
- [129] Y. Wang, C. Zhou, W. Wang, Y.-P. Zhao, *Ind. Eng. Chem. Res.* **2013**, *52*, 4379–4382.
- [130] N. Wang, Q. Xu, S. S. Xu, Y. H. Qi, M. Chen, H. X. Li, B. X. Han, *Sci. Rep.* **2015**, *5*, 16764.
- [131] X. Tian, Y. Li, Z. Chen, Q. Li, L. Q. Hou, J. Y. Wu, Y. S. Tang, Y. F. Li, *Sci. Rep.* **2017**, *7*, 17794.
- [132] P. Thangasamy, M. Sathish, *CrystEngComm* **2015**, *7*, 5895–5899.
- [133] C. C. Nwanonenyi, A. K. Patel, P. Wang, Z. D. Wang, K. Wirth, M. Zaharias, Y.-P. Sun, M. J. Meziani, *J. Supercrit. Fluids* **2021**, *167*, 105035.
- [134] P. Scherrer, *Nachr. Ges. Wiss. Goettingen Math.-Phys. Kl.* **1918**, *2*, 98–100.
- [135] K. Wu, P. Liao, R. Du, Q. Zhang, F. Chen, Q. Fu, *J. Mater. Chem. A* **2018**, *6*, 11863–11873.
- [136] X. Zeng, L. Ye, S. Yu, H. Li, R. Sun, J. Xu, C.-P. Wong, *Nanoscale* **2015**, *7*, 6774–6781.
- [137] J. Han, G. Du, W. Gao, H. Bai, *Adv. Funct. Mater.* **2019**, *29*, 1900412.
- [138] K. Wu, J. Fang, J. Ma, R. Huang, S. Chai, F. Chen, Q. Fu, *ACS Appl. Mater. Interfaces* **2017**, *9*, 30035–30045.
- [139] D. A. Bolon, *IEEE Electr. Insul. Mag.* **1995**, *11*, 10–18.
- [140] Y. Lin, X. Huang, J. Chen, P. Jiang, *High. Volt.* **2017**, *2*, 139–146.
- [141] A. Sahu, D. S. Mondloe, S. Upadhyay, *Int. Res. J. Eng. Tech.* **2017**, *4*, 579–586.
- [142] Z. D. Wang, P. Priego, M. J. Meziani, K. Wirth, S. Bhattacharya, P. Wang, Y.-P. Sun, *Nanoscale Adv.* **2020**, *2*, 2507–2513.
- [143] C. Yu, W. Gong, W. Tian, Q. Zhang, Y. Xu, Z. Lin, M. Hu, X. Fan, Y. Yao, *Compos. Sci. Technol.* **2018**, *160*, 199–207.
- [144] C. Yu, W. Gong, J. Zhang, W. Lv, W. Tian, X. Fan, Y. Yao, *RSC Adv.* **2018**, *8*, 25835–25845.
- [145] M. Tanimoto, T. Yamagata, K. Miyata, S. Ando, *ACS Appl. Mater. Interfaces* **2013**, *5*, 4374–4382.
- [146] J. Zhang, X. Wang, C. Yu, Q. Li, Z. Li, C. Li, H. Lu, Q. Zhang, J. Zhao, M. Hu, Y. Yao, *Compos. Sci. Technol.* **2017**, *149*, 41–47.
- [147] T. Wang, D. Ou, H. Liu, S. Jiang, W. Huang, X. Fang, X. Chen, M. Lu, *ACS Appl. Nano Mater.* **2018**, *1*, 1705–1712.
- [148] J. Chen, X. Huang, Y. Zhu, P. Jiang, *Adv. Funct. Mater.* **2017**, *27*, 1604754.
- [149] X. Wang, P. Wu, *ACS Appl. Mater. Interfaces* **2017**, *9*, 19934–19944.
- [150] Z. Kuang, Y. Chen, Y. Lu, L. Liu, S. Hu, S. Wen, Y. Mao, L. Zhang, *Small* **2015**, *11*, 1655–1659.
- [151] Z. Liu, J. Li, X. Liu, *ACS Appl. Mater. Interfaces* **2020**, *12*, 6503–6515.
- [152] J. Chen, X. Huang, B. Sun, P. Jiang, *ACS Nano* **2019**, *13*, 337–345.
- [153] J. Chen, H. Wei, H. Bao, P. Jiang, X. Huang, *ACS Appl. Mater. Interfaces* **2019**, *11*, 31402–31410.
- [154] Z. Zhu, C. Li, S. E. L. Xie, R. Geng, C.-T. Lin, L. Li, Y. Yao, *Compos. Sci. Technol.* **2019**, *170*, 93–100.
- [155] H. Zhu, Y. Li, Z. Fang, J. Xu, F. Cao, J. Wan, C. Preston, B. Yang, L. Hu, *ACS Nano* **2014**, *8*, 3606–3613.
- [156] J. Wang, Y. Wu, Y. Xue, D. Liu, X. Wang, X. Hu, Y. Bando, W. Lei, *J. Mater. Chem. C* **2018**, *6*, 1363–1369.
- [157] Z. Hu, S. Wang, G. Chen, Q. Zhang, K. Wu, J. Shi, L. Liang, M. Lu, *Compos. Sci. Technol.* **2018**, *168*, 287–295.
- [158] L. Zhou, Z. Yang, W. Luo, X. Han, S. H. Jang, J. Dai, B. Yang, L. Hu, *ACS Appl. Mater. Interfaces* **2016**, *8*, 28838–28843.
- [159] X. Wu, W. Liu, C. Zhang, L. Ren, *Eur. Polym. J.* **2018**, *100*, 12–17.
- [160] J. You, H. Choi, Y. M. Lee, J. Cho, M. Park, S. Lee, J. H. Park, *Compos. B. Eng.* **2019**, *164*, 710–719.
- [161] Y. Wu, Y. Xue, S. Qin, D. Liu, X. Wang, X. Hu, J. Li, X. Wang, Y. Bando, D. Golberg, *ACS Appl. Mater. Interfaces* **2017**, *9*, 43163–43170.
- [162] L. Fu, T. Wang, J. Yu, W. Dai, H. Sun, Z. Liu, R. Sun, N. Jiang, A. Yu, C. Lin, *2D Mater.* **2017**, *4*, 025047.
- [163] M. Loeblein, S. H. Tsang, M. Pawlik, E. J. P. Phua, H. Yong, X. W. Zhang, C. L. Gan, E. H. T. Teo, *ACS Nano* **2017**, *11*, 2033–2044.
- [164] J. Chen, X. Huang, B. Sun, Y. Wang, Y. Zhu, P. Jiang, *ACS Appl. Mater. Interfaces* **2017**, *9*, 30909–30917.
- [165] S. Li, T. Yang, H. Zou, M. Liang, Y. Chen, *High Perform. Polym.* **2017**, *29*, 315–327.
- [166] F. Xiao, S. Naficy, G. Casillas, M. H. Khan, T. Katkus, L. Jiang, H. Liu, H. Li, Z. Huang, *Adv. Mater.* **2015**, *27*, 7196–7203.
- [167] C. Yuan, B. Duan, L. Li, B. Xie, M. Huang, X. Luo, *ACS Appl. Mater. Interfaces* **2015**, *7*, 13000–13006.
- [168] C. Yuan, B. Xie, M. Huang, R. Wu, X. Luo, *Int. J. Heat Mass Transfer* **2016**, *94*, 20–28.
- [169] J. Hou, G. Li, N. Yang, L. Qin, M. E. Grami, Q. Zhang, N. Wang, X. Qu, *RSC Adv.* **2014**, *4*, 44282–44290.
- [170] J. Yu, H. Mo, P. Jiang, *Polym. Adv. Technol.* **2015**, *26*, 514–520.
- [171] X. Cui, P. Ding, N. Zhang, L. Shi, N. Song, S. Tang, *ACS Appl. Mater. Interfaces* **2015**, *7*, 19068–19075.
- [172] T. Gao, Z. Yang, C. Chen, Y. Li, K. Fu, J. Dai, E. M. Hitz, H. Xie, B. Liu, J. Song, B. Yang, L. Hu, *ACS Nano* **2017**, *11*, 11513–11520.
- [173] X. Chen, J. S. K. Lim, W. Yan, F. Guo, Y. N. Liang, H. Chen, A. Lambourne, X. Hu, *ACS Appl. Mater. Interfaces* **2020**, *12*, 16987–16996.
- [174] F. Guo, X. Shen, J. Zhou, D. Liu, Q. Zheng, J. Yang, B. Jia, A. K. Lau, J. Kim, *Adv. Funct. Mater.* **2020**, *30*, 1910826.
- [175] X. He, Y. Wang, *Ind. Eng. Chem. Res.* **2020**, *59*, 1925–1933.
- [176] X. Hou, Y. Chen, L. Lv, W. Dai, S. Zhao, Z. Wang, L. Fu, C.-T. Lin, N. Jiang, J. Yu, *ACS Appl. Nano Mater.* **2019**, *2*, 360–368.

- [177] D. Hu, W. Ma, Z. Zhang, Y. Ding, L. Wu, *ACS Appl. Mater. Interfaces* **2020**, *12*, 11115–11125.
- [178] Z. Hu, S. Wang, Y. Liu, Z. Qu, Z. Tan, K. Wu, J. Shi, L. Liang, M. Lu, *Ind. Eng. Chem. Res.* **2020**, *59*, 4437–4446.
- [179] F. Jiang, S. Cui, C. Rungnim, N. Song, L. Shi, P. Ding, *Chem. Mater.* **2019**, *31*, 7686–7695.
- [180] F. Jiang, S. Cui, N. Song, L. Shi, P. Ding, *ACS Appl. Mater. Interfaces* **2018**, *10*, 16812–16821.
- [181] J. Lao, H. Xie, Z. Shi, G. Li, B. Li, G. Hu, Q. Yang, C. Xiong, *ACS Sustainable Chem. Eng.* **2018**, *6*, 7151–7158.
- [182] C. Lei, K. Wu, L. Wu, W. Liu, R. Du, F. Chen, Q. Fu, *J. Mater. Chem. A* **2019**, *7*, 19364–19373.
- [183] J. Li, F. Li, X. Zhao, W. Zhang, S. Li, Y. Lu, L. Zhang, *ACS Appl. Electron. Mater.* **2020**, *2*, 1661–1669.
- [184] T. Ma, Y. Zhao, K. Ruan, X. Liu, J. Zhang, Y. Guo, X. Yang, J. Kong, J. Gu, *ACS Appl. Mater. Interfaces* **2020**, *12*, 1677–1686.
- [185] T. Morishita, N. Takahashi, *RSC Adv.* **2017**, *7*, 36450–36459.
- [186] A. Pullanchiyodan, K. S. Nair, K. P. Surendran, *ACS Omega* **2017**, *2*, 8825–8835.
- [187] C. V. S. Rosely, A. M. Joseph, A. Leuteritz, E. B. Gowd, *ACS Sustainable Chem. Eng.* **2020**, *8*, 1868–1878.
- [188] C. V. S. Rosely, P. Shaiju, E. B. Gowd, *J. Phys. Chem. B* **2019**, *123*, 8599–8609.
- [189] S. Ryu, H. Oh, J. Kim, *Polymers* **2019**, *11*, 1628.
- [190] N. Song, H. Pan, X. Liang, D. Cao, L. Shi, P. Ding, *J. Mater. Chem. C* **2018**, *6*, 7085–7091.
- [191] K.-H. Su, C.-Y. Su, C.-T. Cho, C.-H Lin, G.-F. Jhou, C.-C. Chang, *Sci. Rep.* **2019**, *9*, 14937.
- [192] J. Sun, Y. Yao, X. Zeng, G. Pan, J. Hu, Y. Huang, R. Sun, J.-B. Xu, C.-P. Wong, *Adv. Mater. Interfaces* **2017**, *4*, 1700563.
- [193] C. Tan, H. Zhu, T. Ma, W. Guo, X. Liu, X. Huang, H. Zhao, Y.-Z. Long, P. Jiang, B. Sun, *Nanoscale* **2019**, *11*, 20648–20658.
- [194] Z. Tian, J. Sun, S. Wang, X. Zeng, S. Zhou, S. Bai, N. Zhao, C.-P. Wong, *J. Mater. Chem. A* **2018**, *6*, 17540–17547.
- [195] J. Wang, D. Liu, Q. Li, C. Chen, Z. Chen, P. Song, J. Hao, Y. Li, S. Fakhrooseini, M. Naebe, X. Wang, W. Lei, *ACS Nano* **2019**, *13*, 7860–7870.
- [196] T. Wang, M. Wang, L. Fu, Z. Duan, Y. Chen, X. Hou, Y. Wu, S. Li, L. Guo, R. Kang, N. Jiang, J. Yu, *Sci. Rep.* **2018**, *8*, 1–8.
- [197] X. Wang, P. Wu, *ACS Appl. Mater. Interfaces* **2019**, *11*, 28943–28952.
- [198] Y. Wang, L. Xu, Z. Yang, H. Xie, P. Jiang, J. Dai, W. Luo, Y. Yao, E. Hitz, R. Yang, L. Hu, *Nanoscale* **2018**, *10*, 167–173.
- [199] Y. Wang, S. Xia, G. Xiao, J. Di, J. Wang, *ACS Appl. Mater. Interfaces* **2020**, *12*, 13156–13164.
- [200] Y. Wang, Z.-X. Low, S. Kim, H. Zhang, X. Chen, J. Hou, J. G. Seong, Y. M. Lee, G. P. Simon, C. H. J. Davies, H. Wang, *Angew. Chem. Int. Ed.* **2018**, *57*, 16056–16061; *Angew. Chem.* **2018**, *130*, 16288–16293.
- [201] K. Wu, J. Wang, D. Liu, C. Lei, D. Liu, W. Lei, Q. Fu, *Adv. Mater.* **2020**, *32*, 1906939.
- [202] K. Wu, L. Yu, C. Lei, J. Huang, D. Liu, Y. Liu, Y. Xie, F. Chen, Q. Fu, *ACS Appl. Mater. Interfaces* **2019**, *11*, 40685–40693.
- [203] Y. Xue, X. Zhou, T. Zhan, B. Jiang, Q. Guo, X. Fu, K. Shimamura, Y. Xu, T. Mori, P. Dai, Y. Bando, C. Tang, D. Golberg, *Adv. Funct. Mater.* **2018**, *28*, 1801205.
- [204] F. Yang, X. Sun, Q. Guo, Z. Yao, *Ind. Eng. Chem. Res.* **2019**, *58*, 18635–18643.
- [205] Y. Yao, J. Sun, X. Zeng, R. Sun, J.-B. Xu, C.-P. Wong, *Small* **2018**, *14*, 1704044.
- [206] Y. Yao, Z. Ye, F. Huang, X. Zeng, T. Zhang, T. Shang, M. Han, W. Zhang, L. Ren, R. Sun, J.-B. Xu, C.-P. Wong, *ACS Appl. Mater. Interfaces* **2019**, *12*, 2892–2902.
- [207] Y. Yao, X. Zeng, R. Sun, J.-B. Xu, C.-P. Wong, *ACS Appl. Mater. Interfaces* **2016**, *8*, 15645–15653.
- [208] Y. Yao, X. Zeng, F. Wang, R. Sun, J.-B. Xu, C.-P. Wong, *Chem. Mater.* **2016**, *28*, 1049–1057.
- [209] Z. Yu, X. Wang, H. Bian, L. Jiao, W. Wu, H. Dai, *PLoS One* **2018**, *13*, e0200842.
- [210] J. Yuan, X. Qian, Z. Meng, B. Yang, Z.-Q. Liu, *ACS Appl. Mater. Interfaces* **2019**, *11*, 17915–17924.
- [211] X.-J. Zha, J. Yang, J.-H. Pu, C.-P. Feng, L. Bai, R.-Y. Bao, Z.-Y. Liu, M.-B. Yang, W. Yang, *Adv. Mater. Interfaces* **2019**, *6*, 1900081.
- [212] R.-C. Zhang, D. Sun, A. Lu, S. Askari, M. Macias-Montero, P. Joseph, D. Dixon, K. Ostrikov, P. Maguire, D. Mariotti, *ACS Appl. Mater. Interfaces* **2016**, *8*, 13567–13572.
- [213] Y. Zhang, W. Gao, Y. Li, D. Zhao, H. Yin, *RSC Adv.* **2019**, *9*, 7388–7399.
- [214] H.-R. Zhao, J.-H. Ding, Z.-Z. Shao, B.-Y. Xu, Q.-B. Zhou, H.-B. Yu, *ACS Appl. Mater. Interfaces* **2019**, *11*, 37247–37255.
- [215] S. Zhou, T. Xu, F. Jiang, N. Song, L. Shi, P. Ding, *J. Mater. Chem. C* **2019**, *7*, 13896–13903.
- [216] L. Chen, K. Li, B. Li, D. Ren, S. Chen, M. Xu, X. Liu, *Compos. Sci. Technol.* **2019**, *182*, 107741.
- [217] L. Chen, C. Xiao, Y. Tang, X. Zhang, K. Zheng, X. Tian, *Ceram. Int.* **2019**, *45*, 12965–12974.
- [218] L. Chen, C. Xiao, Y. Tang, Y. X. Zhang, K. Zheng, X. Tian, *Mater. Res. Express* **2019**, *6*, 075314.
- [219] H.-B. Cho, T. Nakayama, H. Suematsu, T. Suzuki, W. Jiang, K. Niihara, E. Song, N. S. A. Eom, S. Kim, Y. Choa, *Compos. Sci. Technol.* **2016**, *129*, 205–213.
- [220] H. Fang, S.-L. Bai, C.-P. Wong, *Compos. Part A: Appl. Sci. Manufactur.* **2017**, *100*, 71–80.
- [221] H. Fang, S.-L. Bai, C.-P. Wong, *Compos. Commun.* **2016**, *2*, 19–24.
- [222] Y. Feng, G. Han, B. Wang, X. Zhou, J. Ma, Y. Ye, C. Liu, X. Xie, *Chem. Eng. J.* **2020**, *379*, 122402.
- [223] Y. Geng, H. He, Y. Jia, X. Peng, Y. Li, *Polym. Compos.* **2019**, *40*, 3375–3382.
- [224] F. Jiang, X. Cui, N. Song, L. Shi, P. Ding, *Compos. Commun.* **2020**, *20*, 100350.
- [225] Y. Jiang, X. Shi, Y. Feng, S. Li, X. Zhou, X. Xie, *Compos. Part A: Appl. Sci. Manufactur.* **2018**, *107*, 657–664.
- [226] J. Lee, H. Jung, S. Yu, S. Man Cho, V. K. Tiwari, D. B. Velusamy, C. Park, *Chem. Asian J.* **2016**, *11*, 1921–1928.
- [227] Q. Li, Z. Xue, J. Zhao, C. Ao, X. Jia, T. Xia, Q. Wang, X. Deng, W. Zhang, C. Lu, *Chem. Eng. J.* **2020**, *383*, 123101.
- [228] X. Li, Q. Huang, J. Deng, G. Zhang, Z. Zhong, F. He, *J. Power Sources* **2020**, *451*, 227820.
- [229] Y. Li, H. Zhang, X. Yang, G. He, Z. Yang, J. Li, *CrystEngComm* **2019**, *21*, 5461–5469.
- [230] Z. Liu, J. Li, C. Zhou, W. Zhu, *Int. J. Heat Mass Transfer* **2018**, *126*, 353–362.
- [231] X. Ou, X. Lu, S. Chen, Q. Lu, *Eur. Polym. J.* **2020**, *122*, 109368.
- [232] C. Pan, J. Zhang, K. Kou, Y. Zhang, G. Wu, *Int. J. Heat Mass Transfer* **2018**, *120*, 1–8.
- [233] L. Ren, X. Zeng, R. Sun, J.-B. Xu, C.-P. Wong, *Chem. Eng. J.* **2019**, *370*, 166–175.
- [234] H. Ribeiro, J. P. C. Trigueiro, P. S. Owuor, L. D. Machado, C. F. Woellner, J. J. Pedrotti, Y. M. Jaques, S. Kosolwattana, A. Chipara, W. M. Silva, C. J. R. Silva, D. S. Galvão, N. Chopra, I. N. Odeh, C. S. Tiwary, G. G. Silva, P. M. Ajayan, *Compos. Sci. Technol.* **2018**, *159*, 103–110.
- [235] A. Sahoo, H. N. Gayathri, T. P. Sai, P. S. Upasani, V. Raje, J. Berkmans, A. Ghosh, *Nanotechnology* **2020**, *31*, 315706.
- [236] W. Shen, W. Wu, C. Liu, Z. Wang, Z. Huang, *Polym. Adv. Technol.* **2020**, *31*, 1–10.
- [237] A. Shi, Y. Li, W. Liu, J. Lei, L. Xu, Z.-M. Li, *J. Appl. Phys.* **2019**, *125*, 205101.
- [238] L. Wang, W. Wu, D. Drummer, R. Ma, Z. Liu, W. Shen, *J. Appl. Polym. Sci.* **2019**, *136*, 47630.
- [239] X. Wang, P. Wu, *Chem. Eng. J.* **2018**, *348*, 723–731.
- [240] X. Wang, Z. Yu, L. Jiao, H. Bian, W. Yang, W. Wu, H. Xiao, H. Dai, *Nanomaterials* **2019**, *9*, 1051.
- [241] Z. Wang, J. Liu, Y. Cheng, S. Chen, M. Yang, J. Huang, H. Wang, G. Wu, H. Wu, *Nanomaterials* **2018**, *8*, 242.
- [242] Z.-G. Wang, W. Liu, Y.-H. Liu, Y. Ren, Y.-P. Li, L. Zhou, J.-Z. Xu, J. Lei, Z. Li, *Compos. B. Eng.* **2020**, *180*, 107569.
- [243] G. Xiao, J. Di, H. Li, J. Wang, *Compos. Sci. Technol.* **2020**, *189*, 108021.
- [244] C. Xu, M. Miao, X. Jiang, X. Wang, *Compos. Commun.* **2018**, *10*, 103–109.
- [245] Y. Xue, X. Li, H. Wang, F. Zhao, D. Zhang, Y. Chen, *Mater. Des.* **2019**, *165*, 107580.
- [246] G. Yang, B. Wang, H. Cheng, Z. Mao, H. Xu, Y. Zhong, X. Feng, J. Yu, X. Sui, *Int. J. Biol. Macromol.* **2020**, *148*, 627–634.
- [247] N. Yang, X. Zeng, J. Lu, R. Sun, C.-P. Wong, *Appl. Phys. Lett.* **2018**, *113*, 171904.
- [248] S.-Y. Yang, Y.-F. Huang, J. Lei, L. Zhu, Z.-M. Li, *Compos. Part A: Appl. Sci. Manufactur.* **2018**, *107*, 135–143.
- [249] X. Yang, Y. Guo, X. Luo, N. Zheng, T. Ma, J. Tan, C. Li, Q. Zhang, J. Gu, *Compos. Sci. Technol.* **2018**, *164*, 59–64.
- [250] X. Yang, J. Zhu, D. Yang, J. Zhang, Y. Guo, X. Zhong, J. Kong, J. Gu, *Compos. B. Eng.* **2020**, *185*, 107784.
- [251] C.-G. Yin, Y. Ma, Z.-J. Liu, J.-C. Fan, P.-H. Shi, Q.-J. Xu, Y.-L. Min, *Polymers* **2019**, *162*, 100–107.

- [252] D.-L. Zhang, J.-W. Zha, C.-Q. Li, W.-K. Li, S.-J. Wang, Y. Wen, Z.-M. Dang, *Compos. Sci. Technol.* **2017**, *144*, 36–42.
- [253] H. Zhang, R. Huang, Y. Li, H. Li, Z. Wu, J. Huang, B. Yu, X. Gao, J. Li, L. Li, *Polymers* **2019**, *11*, 1335–1348.
- [254] J. Zhang, W. Lei, J. Chen, D. Liu, B. Tang, J. Li, X. Wang, *Polymers* **2018**, *18*, 101–108.
- [255] J. Zhang, W. Lei, D. Liu, X. Wang, *Compos. Sci. Technol.* **2017**, *151*, 252–257.
- [256] Y. Zhang, J. R. Choi, S.-J. Park, *Polymers* **2018**, *143*, 1–9.
- [257] L. Zhao, X. Shi, Y. Yin, B. Jiang, Y. Huang, *Compos. Sci. Technol.* **2020**, *186*, 107919.
- [258] M. Zhu, J. Li, J. Chen, H. Song, H. Zhang, *Comput. Mater. Sci.* **2019**, *164*, 108–115.
- [259] Z. Zhu, P. Wang, P. Lv, T. Xu, J. Zheng, C. Ma, K. Yu, W. Feng, W. Wei, L. Chen, *Polym. Compos.* **2018**, *39*, E1653–E1658.
- [260] D. Zou, X. Huang, Y. Zhu, J. Chen, P. Jiang, *Compos. Sci. Technol.* **2019**, *177*, 88–95.
- [261] X. Zhang, L. Shen, H. Wu, S. Guo, *Compos. Sci. Technol.* **2013**, *89*, 24–28.
- [262] X. Zhang, J. Zhang, L. Xia, C. Li, J. Wang, F. Xu, X. Zhang, H. Wu, S. Guo, *ACS Appl. Mater. Interfaces* **2017**, *9*, 22997–22984.
- [263] Z.-G. Wang, F. Gong, W.-C. Yu, Y.-F. Huang, L. Zhu, L. Jun, J.-Z. Xu, Z.-M. Li, *Compos. Sci. Technol.* **2018**, *162*, 7–13.
- [264] P.-G. Ren, S.-Y. Hou, F. Ren, Z.-P. Zhang, Z.-F. Sun, L. Xu, *Composites Part A* **2016**, *90*, 13–21.
- [265] Y.-F. Huang, Z.-G. Wang, H.-M. Yin, J.-Z. Xu, Y. Chen, J. Lei, L. Zhu, F. Gong, Z.-M. Li, *ACS Appl. Nano Mater.* **2018**, *1*, 3312–3320.
- [266] W. Zhou, S. Qi, H. Li, S. Shao, *Thermochim. Acta* **2007**, *452*, 36–42.
- [267] A. Pakdel, Y. Bando, D. Golberg, *Chem. Soc. Rev.* **2014**, *43*, 934–959.
- [268] Z. Ji, L. Zhang, G. Xie, W. Xu, D. Guo, J. Luo, B. Prakash, *Friction* **2020**, *8*, 813–846.
- [269] C. Androulidakis, K. Zhang, M. Robertson, S. Tawfick, *2D Mater.* **2018**, *5*, 032005.
- [270] D. Gonzalez-Ortiz, C. Salameh, M. Bechelany, P. Miele, *Mater. Today* **2020**, *8*, 100107.
- [271] J. M. Belling, J. Unsworth, *Rev. Sci. Instrum.* **1987**, *58*, 997–1002.
- [272] W. N. dos Santos, J. N. dos Santos, P. Mummary, A. Wallwork, *Polym. Test.* **2010**, *29*, 107–112.
- [273] General Information in ULVAC Technologies, Inc., Thermal Diffusivity Measurement System, <https://www.ulvac.com/components/Thermal-Instruments/Thermoelectric-Testers/LaserPIT>.
- [274] General Information in Erich NETZSCH GmbH & Co. Holding KG, LFA 467 HyperFlash® – Light Flash Apparatus, <https://www.netzscht-thermal-analysis.com/us/products-solutions/thermal-diffusivity-conductivity/lfa-467-hyperflash/>.
- [275] General Information in Quantum Design, Inc. (QD), Physical Property Measurement System, <https://www.qdusa.com/products/ppms.html>.
- [276] General Information in Bethel Co., Ltd., Thermowave Analyzer TA, <https://hrd-thermal.jp/en/apparatus/ta.html>.
- [277] General Information in Hot Disk AB, <https://www.hotdiskinstruments.com/>.
- [278] C.-W. Nan, R. Birringer, D. R. Clarke, H. Gleiter, *J. Appl. Phys.* **1997**, *81*, 6692–6699.
- [279] Y. Liu, C. Hu, J. Huang, B. G. Sumpter, R. Qiao, *J. Chem. Phys.* **2015**, *142*, 244703.
- [280] Y. Wang, C. Yang, Y.-W. Mai, Y. Zhang, *Carbon* **2016**, *102*, 311–318.
- [281] J. Li, J. Chen, M. Zhu, H. Song, H. Zhang, *Appl. Sci.* **2019**, *9*, 2832.

Manuscript received: September 2, 2021

Revised manuscript received: September 30, 2021

Accepted manuscript online: October 8, 2021

Version of record online: November 5, 2021
